



HAL
open science

A Proteomic Analysis Reveals Differential Regulation of the S -Dependent yciGFE(katN) Locus by YncC and H-NS in Salmonella and Escherichia coli K-12

Mélanie Beraud, Annie Kolb, Véronique Monteil, Jacques d'Alayer, Françoise Norel

► **To cite this version:**

Mélanie Beraud, Annie Kolb, Véronique Monteil, Jacques d'Alayer, Françoise Norel. A Proteomic Analysis Reveals Differential Regulation of the S -Dependent yciGFE(katN) Locus by YncC and H-NS in Salmonella and Escherichia coli K-12. *Molecular and Cellular Proteomics*, 2010, 9 (12), pp.2601-2616. 10.1074/mcp.M110.002493 . pasteur-01393398

HAL Id: pasteur-01393398

<https://pasteur.hal.science/pasteur-01393398>

Submitted on 7 Nov 2016

HAL is a multi-disciplinary open access archive for the deposit and dissemination of scientific research documents, whether they are published or not. The documents may come from teaching and research institutions in France or abroad, or from public or private research centers.

L'archive ouverte pluridisciplinaire **HAL**, est destinée au dépôt et à la diffusion de documents scientifiques de niveau recherche, publiés ou non, émanant des établissements d'enseignement et de recherche français ou étrangers, des laboratoires publics ou privés.

A Proteomic Analysis Reveals Differential Regulation of the σ^S -Dependent *yciGFE(katN)* Locus by YncC and H-NS in *Salmonella* and *Escherichia coli* K-12

Mélanie Beraud^{§¶}, Annie Kolb^{§¶}, Véronique Monteil^{§¶}, Jacques D'Alayer^{||}, and Françoise Norel^{§¶‡}

The stationary phase sigma factor σ^S (RpoS) controls a regulon required for general stress resistance of the closely related enterobacteria *Salmonella* and *Escherichia coli*. The σ^S -dependent *yncC* gene encodes a putative DNA binding regulatory protein. Application of the surface-enhanced laser desorption/ionization-time of flight (SELDI-TOF) ProteinChip technology for proteome profiling of wild-type and mutant strains of *Salmonella enterica* serovar Typhimurium revealed potential protein targets for YncC regulation, which were identified by mass spectrometry, and subsequently validated. These proteins are encoded by the σ^S -dependent operon *yciGFEkatN* and regulation of their expression by YncC operates at the transcriptional level, as demonstrated by gene fusion analyses and by *in vitro* transcription and DNase I footprinting experiments with purified YncC. The *yciGFE* genes are present (without *katN*) in *E. coli* K-12 but are poorly expressed, compared with the situation in *Salmonella*. We report that the *yciGFE(katN)* locus is silenced by the histone-like protein H-NS in both species, but that σ^S efficiently relieves silencing in *Salmonella* but not in *E. coli* K-12. In *Salmonella*, YncC acts in concert with σ^S to activate transcription at the *yciG* promoter (*pyciG*). When overproduced, YncC also activated σ^S -dependent transcription at *pyciG* in *E. coli* K-12, but solely by countering the negative effect of H-NS. Our results indicate that differences between *Salmonella* and *E. coli* K-12, in the architecture of *cis*-acting regulatory sequences upstream of *pyciG*, contribute to the differential regulation of the *yciGFE(katN)* genes by H-NS and YncC in these two enterobacteria. In *E. coli*, this locus is subject to gene rearrangements and also likely to horizontal gene transfer, consistent with its repression by the xenogeneic silencer H-NS. *Molecular & Cellular Proteomics* 9: 2601–2616, 2010.

In eubacteria, transcription depends on a multisubunit RNA polymerase (RNAP) consisting of a catalytically active core enzyme (E) with a subunit structure $\alpha_2\beta\beta'\omega$, that associates with any one of several σ factors to form different holoenzyme ($E\sigma$) species. The σ subunit is required for specific promoter binding, and different σ factors direct RNAP to different classes of promoters, thereby modulating gene expression patterns (1). The RNA polymerase holoenzyme containing the σ^{70} subunit is responsible for the transcription of most genes during exponential growth (1). When cells enter stationary phase or are under specific stress conditions during exponential growth, σ^S , encoded by the *rpoS* gene, becomes more abundant, associates with the core enzyme, and directs the transcription of genes essential for the general stress response (1–3). In the closely related Enterobacteria *Salmonella* and *Escherichia coli*, σ^S is required for stationary phase survival, stress resistance, and biofilm formation. It is also involved in the virulence of *Salmonella enterica* serovar Typhimurium (S. Typhimurium) (4).

Transcriptome analyses in *S. Typhimurium* and *E. coli* K-12 have shown that *rpoS* controls more than 300 genes, 40% of which are of unknown function (3, 5, 6). A large fraction of σ^S -controlled genes encode putative regulators and signal transducing factors, suggesting that σ^S controls a complex network with regulatory cascades and signal input at levels downstream of σ^S itself. We previously used a bank of *S. Typhimurium* mutants to identify σ^S -regulated genes (7). One of these genes, the *yncC* gene (7), encoded a putative DNA binding protein of the GntR/FadR family of bacterial regulators (8–10). To further investigate the function of the *yncC* gene, we decided to characterize the proteome of the *Salmonella yncC* mutant by the surface-enhanced laser desorption/ionization-time of flight (SELDI-TOF¹) ProteinChip technology.

The SELDI-TOF method is based on the selective protein retention on a solid-phase chromatographic chip surface and successive analysis by simple laser desorption/ionization mass spectrometry (11). Because of its high-throughput nature and experimental simplicity, this technology has been widely used for protein profiling of tissues and biomarker discovery (11) and unpublished work from our laboratory re-

From the [§]Institut Pasteur, Unité de Génétique moléculaire, Département de Microbiologie F-75015 Paris, France, [¶]CNRS, URA2172, F-75015 Paris, France, ^{||}Institut Pasteur, Plate-Forme d'Analyse et de Microséquençage des Protéines, Génopole, F-75015 Paris, France

Received July 1, 2010, and in revised form, July 29, 2010

Published, MCP Papers in Press, August 16, 2010, DOI 10.1074/mcp.M110.002493

vealed the efficiency of this in characterizing the RpoS-dependent proteome of *Salmonella*. In the present study, potential protein targets for YncC regulation in *Salmonella* were revealed by SELDI-TOF, identified and subsequently validated by *in vivo* and *in vitro* analyses. These proteins are encoded by the *Salmonella yciGFEkatN* operon controlled by σ^S (12). The binding of YncC upstream of the *yciG* promoter and its effects on σ^S -dependent transcription were investigated.

During the course of this work, it was reported that *mcbR*, the ortholog of *yncC* in *E. coli* K-12, represses the transcription of the *ybiM* gene, which prevents overproduction of colanic acid and subsequent inhibition of biofilm formation (13). We report here that *ybiM* is not present in *Salmonella*, prompting investigation of the possibility that these two orthologs perform different regulatory functions in *E. coli* K-12 and *Salmonella* by studying activation of *yciGFE* gene expression by YncC/McbR in *E. coli* K-12. The results reveal differential regulation of the *yciGFE(katN)* locus by YncC and H-NS (the Histone-like Nucleoid Structuring protein, 14–16) in these two closely related bacteria.

EXPERIMENTAL PROCEDURES

Bacterial Strains, Plasmids, and Growth Conditions—Strains and plasmids are listed in Table I. Bacteriophage P22HT105/1int was used to transfer mutations between *Salmonella* strains by transduction (26). Green plates, for screening for P22-infected cells or lysogens, were prepared as described previously (27). Bacteriophage P1 transduction (28) was used to construct mutants in *E. coli* K-12 using mutants available from the KEIO collection (20) (Table I). Strains were routinely cultured in Luria Bertani medium (LB)¹ (17). Antibiotics were used at the following concentrations: ampicillin, 100 μ g/ml; carbenicillin, 100 μ g/ml; chloramphenicol, 15 μ g/ml for the chromosomal resistance gene and 30 μ g/ml for the plasmid resistance gene; kanamycin, 50 μ g/ml; and tetracycline 20 μ g/ml.

DNA Manipulations and Sequence Analysis—Standard molecular biology techniques were used (17). Oligonucleotides were obtained from Sigma-Aldrich (France). DNA sequencing was performed by Beckman Coulter Genomics (France). DNA and amino acid sequence analyses were conducted using the BLAST programs at the National Center for Biotechnology Information (<http://www.ncbi.nlm.nih.gov/>), the Genome Center at Washington University (<http://genome.wustl.edu/genomes/>), and the Sanger Institute (<http://www.sanger.ac.uk/Projects/Salmonella/>). Other Web sites for sequence analyses were <http://www.genome.jp/kegg> and <http://enterix.cbcb.umd.edu/>. Physico-chemical parameters of protein sequences were predicted using ProtParam (ExPASy Web site).

Construction of Plasmids—The nucleotide sequence of a PCR-amplified *yncC* gene (STM1588) from *S. Typhimurium* ATCC14028 revealed that it is identical to that in *S. Typhimurium* LT2 (<http://genomeold.wustl.edu/projects/bacterial/styphimurium/>) and to that in the recently published genome sequence of ATCC14028 (GenBank CP001363) (29). A 1.3 kb BamHI fragment carrying the kanamycin resistance cartridge from pUC4K was ligated into the BamHI restriction site in pACYC184, resulting in pACK. pACK*yncC* was con-

structed using primers YncC-E1 and YncC-E2 (Table II) to amplify the promoter-less *yncC* gene from ATCC14028 total DNA by PCR. EcoRI restriction sites were incorporated at its 5' and 3' ends. Following digestion with EcoRI, the fragment was inserted into the EcoRI site of pACK to give pACK*yncC* (the *yncC* and *cat* genes are in the same orientation and the *yncC* gene is likely transcribed from the *cat* promoter). The nucleotide sequence of the *yncC* insert in pACK*yncC* was verified by DNA sequencing. *pyncC_{HIS}*, which expresses an N-terminal His₆ fusion to the *yncC* gene product under the control of the pQE30 IPTG-inducible promoter, was constructed as follows. Primers YncC-H3 and YncC-H5 (Table II) were used to amplify the *yncC* gene from ATCC14028 total DNA by PCR. BamHI and HindIII restriction sites were incorporated at its 5' and 3' ends, respectively. Following digestion with BamHI and HindIII, the PCR-amplified fragment was ligated into the BamHI and HindIII sites of pQE30. The nucleotide sequence of the *yncC* insert in *pyncC_{HIS}* was verified. Construction of plasmid for *in vitro* transcription was as follows. The *E. coli yciG* fragment (extending from -227 to +66 relative to the transcription start) was synthesized from primers M91 and M92 and the *S. Typhimurium yciG* fragment (-184 to +48) from primers M47 and M48bis. The fragments were cleaved by EcoRI and BamHI and inserted into the pJCD01 vector cleaved by EcoRI and BamHI, leading to plasmids pJCD*yciG* and pJCD*katN*.

Construction of the Δ *yncC* Δ *hns* and Δ *yci* Mutants of *S. Typhimurium*—Chromosomal deletions in the *yncC*, *hns* and *yciGFEkatN* loci of *Salmonella* ATCC14028 were generated using PCR-generated linear DNA fragments and the λ Red recombination method as described by Datsenko and Wanner (30). Briefly, 63–66 nt primers with 43–46 nt homology with the gene of interest on the 5' end of the primer and 20 nt homology with the FLP recognition target flanked antibiotic resistance cassette of plasmid pKD3 at the 3' end (sequences given in 30) were used. The primer pairs, YncC-P1 and YncC-P2, Hns-P1 and Hns-P2, YciG-P1 and KatN-P2 (Table II) were used for disruption of the *yncC*, *hns*, and *yciGFEkatN* operon, respectively. ATCC14028 containing the plasmid pKD46, which carries the λ recombination genes *gam*, *bet*, and *exo* under control of the *araBAD* promoter (30) was grown overnight at 30 °C, diluted in LB carbenicillin containing L-arabinose 1 mM and grown to an OD₆₀₀ of 0.5. Electrocompetent cells were prepared, transformed with the PCR-generated linear fragments and plated on LB containing chloramphenicol (15 μ g/ml) and incubated at 37 °C. The resulting colonies were characterized using a combination of PCR reactions using locus-specific primers and common test primers (30). Finally, isogenic strains were constructed by P22 mediated transduction of the mutations into the appropriate strains. When required, the chloramphenicol resistance cassette was eliminated using a temperature-sensitive helper plasmid pCP20, which encodes the FLP recombinase (30). Because the *hns* mutants were very sick and might accumulate compensatory mutations, they were constructed freshly for each experiment.

Construction of a Chromosomal *yciE-lacZ* Transcriptional Fusion in *E. coli* K-12—A single copy *yciE-lacZ* transcriptional fusion was constructed from mutant MC4100*yciE* using conditional plasmids containing promoter-less *lacZ* genes and the FLP recognition target site as described (31). PCR assays were then used to ensure integration of the plasmids in the correct location and to determine the presence of multiple plasmid integrants (using common test primers, such as those described in (31)). Locus-specific flanking primers were also used to amplify junction fragments that were subsequently analyzed by DNA sequencing. Isogenic strains were constructed by P1 mediated transduction of the mutations into the appropriate strains.

Protein Profiling by SELDI-TOF-MS—Bacteria were grown in LB for 18 h at 37 °C. Cells were harvested and cell pellets obtained from 100 ml of culture were resuspended in 20 ml phosphate buffer 50 mM pH 7 and disrupted in a Cell Disrupter (Constant Systems, Daventry, UK).

¹ The abbreviations used are: LB, Luria Bertani; SELDI-TOF-MS, surface-enhanced laser desorption/ionization -time of flight-mass spectrometry; s/n, signal to noise.

TABLE I
Bacterial strains and plasmids used in this study

Strain or plasmid	Characteristics	Source or reference ^a
Escherichia coli		
JM109	<i>recA1 supE44 endA1 hsdR17 gyrA96 relA1 thi</i> $\Delta(lac-proAB)$ F'(traD36 proAB ⁺ lacI ^q lacZ Δ M15)	17
MG1655	F ⁻ λ^- <i>ilvG rfb-50 rph-1</i>	18
MC4100	$\Delta(lacIPOZYA)X74$, <i>galU</i> , <i>galK</i> , <i>strA-R</i> , $\Delta(ara-leu)$	Laboratory stock
MC1061	<i>araD139</i> $\Delta(ara-leu)-767$ $\Delta(lacIPOZY)X74$ <i>rpsL galU galK</i>	17
popH118	F ⁻ <i>araD139</i> $\Delta(argF-lac)-U169$ <i>rpsL150 relA1 flbB5301</i> $\Delta_{\mu\alpha\lambda A510\phi}$ (<i>malQ-lacZ</i>) <i>hyb110</i> <i>deoC ptsF25 rbsR</i> $\Delta hns-118$	19
JW5437	$\Delta rpoS::Km$	20
JW1445	$\Delta yncC::Km$	20
JW1249	$\Delta yciE::Km$	20
JW1250	$\Delta yciF::Km$	20
MG1655 <i>yciE</i>	MG1655 $\Delta yciE::Km$	
MG1655 <i>yciF</i>	MG1655 $\Delta yciF::Km$	
MG1655 <i>hns</i>	MG1655 $\Delta hns-118$	
MG1655 <i>yciEhns</i>	MG1655 $\Delta yciE::Km$ $\Delta hns-118$	
MG1655 <i>yciFhns</i>	MG1655 $\Delta yciF::Km$ $\Delta hns-118$	
MC4100 <i>yciE</i>	MC4100 $\Delta yciE::Km$	
MC4100 <i>hns</i>	MC4100 $\Delta hns-118$	
MC1061 <i>hns</i>	MC1061 $\Delta hns-118$	
MC4100 <i>rpoS</i>	MC4100 $\Delta rpoS::Km$	
MC4100 <i>yciE-lacZ</i>	MC4100 <i>yciE-lacZY</i>	
MC4100 <i>mcbR yciE-lacZ</i>	MC4100 $\Delta yncC yciE-lacZ$	
MC4100 <i>rpoS yciE-lacZ</i>	MC4100 $\Delta rpoS yciE-lacZY$	
MC4100 <i>hns yciE-lacZ</i>	MC4100 <i>yciE-lacZY</i> $\Delta hns-118$	
MC4100 <i>rpoShns yciE-lacZ</i>	MC4100 $\Delta rpoS yciE-lacZ$ $\Delta hns-118$	
MC4100 <i>mcbRhns yciE-lacZ</i>	MC4100 $\Delta yncC yciE-lacZ$ $\Delta hns-118$	
Salmonella serovar Typhimurium		
ATCC14028	Wild-type	ATCC ^b
ATCC-F12	ATCC14028 <i>yncC::Tn5B21-F12</i>	7, 21
ATCC-F1	ATCC14028 <i>yciF::Tn5B21-F1</i>	7, 21
ATCC <i>katN-lacZ</i>	ATCC14028 <i>katN::Tn5B21-G57</i>	7, 21
ATCC <i>rpoS</i>	ATCC14028 $\Delta rpoS::Cm$	22
ATCC <i>yncC</i>	ATCC14028 $\Delta yncC::Cm$	
ATCC Δyci	ATCC14028 $\Delta yciGFEkatN::Cm$	
ATCC <i>hns</i>	ATCC14028 $\Delta hns::Cm$	
ATCC <i>yncC katN-lacZ</i>	ATCC14028 $\Delta yncC::Cm$ <i>katN::Tn5B21-G57</i>	
ATCC <i>rpoS katN-lacZ</i>	ATCC14028 $\Delta rpoS::Cm$ <i>katN::Tn5B21-G57</i>	21
ATCC <i>hns katN-lacZ</i>	ATCC14028 $\Delta hns::Cm$ <i>katN::Tn5B21-G57</i>	
ATCC <i>hnsrpoS katN-lacZ</i>	ATCC14028 $\Delta rpoS$ $\Delta hns::Cm$ <i>katN::Tn5B21-G57</i>	
ATCC <i>hnsyncC katN-lacZ</i>	ATCC14028 $\Delta yncC$ $\Delta hns::Cm$ <i>katN::Tn5B21-G57</i>	
ATCC2922K	ATCC14028 $\Delta STM2922::Km$	21
ATCC2922K <i>rpoS</i>	ATCC2922K $\Delta rpoS::Cm$	21
ATCC2922K <i>hns</i>	ATCC2922K $\Delta hns::Cm$	
ATCC <i>rpoS</i> _{LT2}	ATCC2922K <i>rpoS</i> _{LT2}	21
ATCC <i>rpoS</i> _{LT2} <i>hns katN-lacZ</i>	ATCC2922K <i>rpoS</i> _{LT2} $\Delta hns::Cm$	
ATCC2922K <i>katN-lacZ</i>	ATCC2922K <i>katN::Tn5B21-G57</i>	21
ATCC2922K <i>rpoS katN-lacZ</i>	ATCC2922K $\Delta rpoS::Cm$ <i>katN::Tn5B21-G57</i>	21
ATCC2922K <i>hns katN-lacZ</i>	ATCC2922K $\Delta hns::Cm$ <i>katN::Tn5B21-G57</i>	
ATCC2922K <i>yncC katN-lacZ</i>	ATCC2922K $\Delta yncC::Cm$ <i>katN::Tn5B21-G57</i>	
ATCC <i>rpoS</i> _{LT2} <i>katN-lacZ</i>	ATCC2922K <i>rpoS</i> _{LT2} <i>katN::Tn5B21-G57</i>	21
ATCC <i>rpoS</i> _{LT2} <i>hns katN-lacZ</i>	ATCC2922K <i>rpoS</i> _{LT2} $\Delta hns::Cm$ <i>katN::Tn5B21-G57</i>	
ATCC <i>rpoS</i> _{LT2} <i>yncC katN-lacZ</i>	ATCC2922K <i>rpoS</i> _{LT2} $\Delta yncC::Cm$ <i>katN::Tn5B21-G57</i>	
ATCC <i>rpoS</i> _{LT2} <i>hnsyncC katN-lacZ</i>	ATCC2922K <i>rpoS</i> _{LT2} $\Delta yncC$ $\Delta hns::Cm$ <i>katN::Tn5B21-G57</i>	

TABLE I—continued

Strain or plasmid	Characteristics	Source or reference ^a
Plasmids		
pACYC184	Cloning vector, Cm ^R , Tet ^R	23
pACK	pACYC184::Km, Cm ^R , Km ^R	
pACK _{<i>yncC</i>}	pACK with the promoterless <i>yncC</i> gene cloned into the <i>cat</i> gene (<i>yncC</i> is transcribed from the <i>cat</i> promoter), Km ^R	
pUC4K	Source of Km resistance cartridge	Pharmacia
pQE30	Vector for expression of His-tagged proteins, Cb ^R	Qiagen
<i>pync</i> _{HIS}	pQE30:: <i>yncC</i> expresses a His ₆ -YncC protein, Cb ^R	
<i>pmcbR</i> _{HIS}	pCA24N P _{T5-lac} :: <i>yncC</i> , Cm ^R , lacI ^q	24
pCABg	<i>pmcbR</i> _{HIS} deleted from the <i>Bgl</i> I fragment carrying <i>yncC</i>	
pJCD01	Cloning vector for promoter fragments upstream of the <i>rmB</i> T1 terminator	25
pJCD _{<i>katN</i>}	pJCD01 containing the <i>yciG</i> _{STM} promoter	21
pJCD _{<i>yciG</i>}	pJCD01 containing the <i>yciG</i> _{ECCO} promoter	

^a This study, unless otherwise noted.

^b American Type Culture Collection.

TABLE II
Primers used in this study

Primer	Sequence
YncC-P1	CGATTGCGATGTTGTTCTGCCAAGAGGTGAAGGAAGGAAAATGGTGTAGGCTGGAGCTGCTTC
YncC-P2	GAATCCCCGCTATTGATAAGTCATAGTTTCATGAAAGTTACATCATATGAATATCCTCCTTAG
YciG-P1	ACCGATTTTTTCAGCAAGCAACGAGACAGGAGAAAATAATATGGGTGTAGGCTGGAGCTGCTTC
KatN-P2	AAGGACATGACACACGGATTTTACTTGTGCGGAACCTACTTGTCCATATGAATATCCTCCTTAG
Hns-P1	CCCCAATATAAGTTTGAGATTACTACAATGAGCGAAGCAGCTGTAGGCTGGAGCTGCTTC
Hns-P2	CATCCAGGAAGTAAATATTCTTGTATCAGGAAATCTTCCATATGAATATCCTCCTTAG
YncC-E1	CGGGACTCGATTGCGAATTCGTTCTGCCAAGAGGT
YncC-E2	GAATCCCCGCTATTGAGAATTCATAGTTTCATGAAAGT
YncC-H3	GCCAAGAGGTGAAGGAGGATCCATGCCGGGTACGGA
YncC-H5	AGTCAAAGCTTCATGAAAGTTACATGAAGTACTGAT
E7 (pJCD01)	CTGGCAGATGCGTCTTCCG
J7 (pJCD01)	GGATTGTCTCTACTCAGGAG
M47 (<i>yciG</i> _{STM} up)	GGCGAATTCAGGGCCGAGATAGTG
M48bis (<i>yciG</i> _{STM} down)	GGCGAATTCAGGGCCGAGATAGT
M57bis (<i>yciG</i> _{STM} middle)	CCCGAATTCGGTAAATCACAACTATTTCCTCG
M91 (<i>yciG</i> _{COLI} up)	GCGGAATTCGGTAAATCACAACTATTTCCTCG
M92 (<i>yciG</i> _{COLI} down)	CCGGATCCATGTTATTCTCCCGTTGCG

The cell debris were removed by centrifugation. Protein concentrations in the supernatants were determined using the DC Protein Assay kit (Bio-Rad) and adjusted to a concentration of 1 μg/μl in phosphate buffer 50 mM pH 7. These cytosol extracts were stored at -70 °C. The SELDI analysis was performed using 10 μg crude cytosol extracts of *Salmonella* and *E. coli* strains. For each strain, three independent cultures were used to prepare cytosol extracts and each extract was spotted in duplicate on the ProteinChip array. A strong anion exchange ProteinChip array (Q10, Bio-Rad), for which the complementary resin Q Ceramic HYPERD F (BioSeptra-Pall, Cergy St Christophe, France) can be used for protein purification, was employed to capture negatively charged proteins. Before loading the cell extracts, the Q10 array was equilibrated once for 10 min with 150 μl of buffer T50 (50 mM Tris-HCl pH 9), and once for 5 min with 100 μl of buffer T50 containing 0.1% Triton, using a bioprocessor. Bacterial extracts (10 μg) were diluted in 100 μl of T50 containing 0.1% Triton and incubated on the chips for 1 h at room temperature under shaking. Then, the chips were washed: first for 10 min with 100 μl of T50 containing 0.1% Triton, second, twice for 5 min with 150 μl of T50 and finally twice with double-distilled H₂O. The samples were then air-dried. Then, 0.7 μl of sinapinic acid (Bio-Rad) saturated in freshly prepared

50% acetonitrile-0.5% trifluoroacetic acid was applied twice on each spot and the spots were air dried. Molecules retained on the surfaces were visualized by reading the spots of each array in a SELDI-TOF-MS reader (PSC4000; Ciphergen Biosystems, Copenhagen, Denmark). Spectra were generated by seven shots on 36 pixels at laser energy varying between 2600 and 4500 nJ and an accelerating voltage of 25 kV in positive mode with automatic data collection software 3.0 program. External mass calibration was performed on one spot of each array by using ubiquitin (8564.8 Da), cytochrome C (12,230.9 Da), β-lactoglobulin A (18,363.3 Da), horseradish peroxidase (43,240.0 Da), Conalbumine (77,490.0 Da), and IgG bovine (147,300.0 Da).

Raw spectra were processed and analyzed with the Ciphergen Express data manager software version 3.0 (CE; Ciphergen Biosystems). Spectra were externally calibrated with cytochrome C (bovine) (12,230.9 + 1H), β-lactoglobulin A (bovine) (18,363.3 + 1H) and horseradish peroxidase (43,240.0 + 1H). The baseline was established using a smoothing of three points and a width of five times expecting peak width and spectral intensities were normalized by total ion current. Consistent peak sets of similar mass across the spectra were generated with CiphergenExpress Cluster Wizard. This

Wizard operates in three passes across the spectra. The first pass performs peak detection at high signal-to-noise (s/n) ratio to pick out well-defined peaks as starting points for forming clusters. A second pass selects lower s/n ratio peaks, within a mass window defined around the first pass peaks. The algorithm completes the clusters in a third pass by creating artificial peaks where none were detected in the first two passes, at the exact center of clusters. In this analysis, unless otherwise specified, the first pass was performed with an s/n threshold of five, and the second pass with an s/n threshold of two, in a 0.5% width mass window. Clusters were assembled between 5000 and 40,000 Da. The cluster lists contained normalized peak intensity values for each sample within a group and *p* values were calculated between the medians of the peak intensities to detect significant differences in abundance for particular proteins.

Proteome Fractionation on Q Ceramic HYPERD F—A volume of 80 μ l of Q Ceramic HYPERD F beads (BioSeptra-Pall Corporation) were equilibrated three times in buffer T50, centrifuged, and resuspended in 10 ml of T50 containing 0.1% Triton. Bacterial cytosol extracts (8 mg in 4 ml) were incubated with the beads for 2 h at 4 °C on a rotative shaker and centrifuged. Beads were washed twice in T50 containing 0.1% Triton, and then twice in T50 and finally once in Tris-HCl 5 mM pH 9.0. Proteins captured on the beads were eluted successively in 100 μ l HEPES 50 mM pH 8.0, 100 μ l phosphate buffer 50 mM pH 7.0, 100 μ l MES 50 mM pH 6.0, 100 μ l sodium acetate 50 mM pH 5.0, 100 μ l sodium acetate 50 mM pH 4.0, 100 μ l sodium acetate 50 mM pH 3.4, and finally 100 μ l sodium acetate 50 mM NaCl 1 M pH 3.4. Proteins in the eluted fractions (25 μ l) were separated by SDS-PAGE on a 12.5% acrylamide gel. The gel was stained with Coomassie blue.

Identification of the *YciF* and *YciE* Proteins by Mass Spectrometry—Mass spectrometry analyses have been conducted at the PF3 Proteomic platform (Abdelkader Namane, Institut Pasteur, France).

Sample Preparation—One-dimensional gel bands were excised from gels and collected in 96-well plate. Destaining, reduction, alkylation, trypsin digestion of the proteins followed by peptide extraction were carried out with the Progest Investigator (Genomic Solutions, Ann Arbor, MI). Following the desalting step (C18- μ ZipTip, Millipore) peptides were eluted directly using the ProMS Investigator, (Genomic Solutions) onto a 96-well stainless steel matrix-assisted laser desorption ionization target plate (Applied Biosystems/MDS SCIEX, Framingham, MA) with 0.5 μ l of CHCA matrix (5 mg/ml in 70% acetonitrile/30% H₂O/0.1% trifluoroacetic acid).

MS and MS/MS Analysis—Raw data for protein identification were obtained on the 4800 Proteomics Analyzer (Applied Biosystems) and analyzed by GPS Explorer 2.0 software (Applied Biosystems/MDS SCIEX). For positive-ion reflector mode spectra 3000 laser shots were averaged. For MS calibration, autolysis peaks of trypsin ($[M+H]^+ = 842.5100$ and 2211.1046) were used as internal calibrates. Monoisotopic peak masses were automatically determined within the mass range 800–4000 Da with a signal to noise ratio minimum set to 20. Up to 12 of the most intense ion signals were selected as precursors for MS/MS acquisition excluding common trypsin autolysis peaks and matrix ion signals. In MS/MS positive ion mode, 4000 spectra were averaged, collision energy was 2 kV, collision gas was air and default calibration was set using the Glu¹-Fibrino-peptide B ($[M+H]^+ = 1570.6696$) spotted onto 14 positions of the matrix-assisted laser desorption ionization target. Combined PMF and MS/MS queries were performed using the MASCOT search engine 2.1.04 (Matrix Science, London, UK) embedded into GPS-Explorer Software 2.0 (Applied Biosystems/MDS SCIEX) on the National Center for Biotechnology Information database 20070518 (4927571 sequences, 17002359384 residues) with the following parameter settings: 50 ppm peptide mass accuracy, specific trypsin cleavage (K/R), one missed cleavage allowed, carbamidomethylation set as fixed modification,

oxidation of methionines was allowed as variable modification, MS/MS fragment tolerance was set to 0.3 Da. Protein hits with MASCOT Protein score ≥ 79 and a GPS Explorer Protein confidence index $\geq 95\%$ were used for further manual validation.

Enzymatic Assays— β -galactosidase activity was measured as described by Miller (32) and is expressed in Miller units.

Electrophoresis and Immunoblot Analysis of Proteins—Whole-cell extracts were prepared and SDS-polyacrylamide gel electrophoresis was carried out as described by Silhavy *et al.* (28). The amount of protein in whole-cell lysates was determined using the DC Protein Assay kit (Bio-Rad). Equal amounts of protein were loaded in each slot. The molecular sizes of the proteins were estimated using molecular size standards (Fermentas, France). Rabbit antibodies against the σ^S protein of *S. enterica* serovar Typhimurium were from Coynault *et al.* (33). Mouse monoclonal IgG1 penta-His antibody (Qiagen) was used to detect His-tagged proteins. Proteins were transferred to Amersham Biosciences Hybond P membranes (GE Healthcare) and incubated with the antibodies as previously described (33). Bound antibodies were detected using secondary anti-rabbit (for σ^S detection) and anti-mouse (for His-tag detection) antibodies linked to peroxidase and the Amersham Biosciences ECL plus Western blotting detection system kit (GE Healthcare).

Overproduction and Purification of His₆-YncC—A 500-ml culture of JM109 carrying *pyncC_{HIS}* was grown in LB containing 100 μ g/ml carbenicillin at 28 °C to an optical density of 0.6 and then supplemented with 1 mM isopropyl- β -D-thiogalactoside. Following 4 h, cells were harvested, washed, resuspended in 10 ml of phosphate buffer (50 mM Na₂HPO₄ pH 8) and lysed by high pressure cell disruption. The extract was supplemented with 300 mM NaCl and centrifuged at $15,000 \times g$ for 30 min at 4 °C. The supernatant was added to 2.5 ml of Ni-NTA agarose (Qiagen) and gently mixed for 180 min. The slurry was packed into an Econo-Pac column (Bio-Rad), washed with 25 ml buffer A (50 mM Na₂HPO₄ pH 8, 300 mM NaCl) containing 20 mM imidazole. His₆-YncC was eluted with buffer A containing 250 mM imidazole, dialyzed against buffer B (20 mM Tris-HCl pH 8, 20 mM NaCl, 1 mM dithiothreitol), loaded onto a Hitrap Q anion exchange-column (1 ml; GE Healthcare). Following washing with 10 ml buffer B His₆-YncC was eluted from the column with a linear gradient from 0.02 to 1 M NaCl between 0.15 M and 0.2 M NaCl. The pooled fractions were dialyzed against buffer C (10 mM Tris-HCl pH 7.9, 100 mM NaCl, 50% glycerol, 1 mM dithiothreitol). The purification yield was 3 mg of His₆-YncC, as determined by Bradford assay.

Labeled DNA Fragments—Primers were ³²P-labeled at their 5' ends using phage T4 polynucleotide kinase and [γ -³²P]-ATP (800 Ci/mmol). The *E. coli yciG* promoter fragment was generated by PCR using MG1655 chromosomal DNA and primers M91 and M92. For nontemplate strand labeling, [³²P]-labeled primer M91 was used with unlabeled primer M92. The *S. Typhimurium yciG* fragments were generated by PCR using *pJCDkatN* as template (21) and [³²P]-labeled primer E7 and M48bis for nontemplate strand labeling and [³²P]-labeled M48bis and E7 for template strand labeling. The fragments were then purified on a glass fiber column (High Pure PCR Product Purification Kit from Roche Diagnostics, Neuilly, France).

DNase I Footprinting—The [³²P]-labeled fragments were incubated for 20 min in a final volume of 15 μ l with increasing concentrations of His₆-YncC in buffer C (40 mM Hepes pH 8.0, 10 mM MgCl₂, 100 mM potassium glutamate, 5 mM dithiothreitol and 500 μ g/ml bovine serum albumin). 1.5 μ l of a 1 μ g/ml DNase I solution (Worthington) in buffer D (10 mM Tris-HCl pH 8.0, 10 mM MgCl₂, 10 mM calcium chloride, 125 mM potassium chloride) were then added and incubated for 10 s when the labeled fragment was alone, or for 10 to 40 s depending on YncC concentrations (expressed in dimers). The reaction was stopped with phenol, as described (34), and loaded on a 7.5% sequencing polyacrylamide gel. Protected bands were identified by comparing the

migration of the same fragment treated for the A+G sequencing reaction (35). The *E. coli* H-NS protein was a gift from Sylvie Rimsky and its concentration is expressed in monomers. In the competitive binding assays with H-NS and His₆-YncC, the proteins were first mixed and incubated with promoter fragments at 30 °C for 20 min in buffer C × 0.5 before DNase I attack.

In Vitro Transcription—The DNA fragments were prepared from pJCD01 derivatives containing the promoter fragments cloned upstream of the *rrnB1* terminator using primers E7 and J7 (25). A shorter *S. Typhimurium yciG* fragment (−61 to +48) that does not harbor the YncC binding site was generated using pJCD*katN* and primers M57bis and J7 (21). The *katE* promoter fragment was described in Robbe-Saule *et al.* (21). E σ^S RNA polymerase was reconstituted from core RNA polymerase either wild-type (Epicenter Biotechnologies, Madison, WI) or harboring α subunits truncated in the C-terminal domains (36), and His- σ^S prepared from *S. Typhimurium* (37). Different amounts of YncC were incubated for 20 min at 37 °C with promoter fragments (at a final concentration of 10 nM) in buffer C before E σ^S RNA polymerase addition (E: 15 nM, σ^S : 60 nM) and incubation was prolonged for 20 min before addition of the heparin/XTP mixture (21). H-NS was first incubated with DNA templates (20 nM) for 20 min at 30 °C in 5 μ l buffer A. A 5- μ l aliquot of a mixture containing RNA polymerase with or without YncC (E: 60 nM, σ^S : 240 nM, YncC: 500 nM) was then added. Incubation was prolonged for 10 min before adding 5 μ l of a heparin/XTP mixture (450 μ M ATP, CTP, and GTP and 45 μ M [α -³²P]-UTP). The reaction was stopped following 10 min by adding 15 μ l of formamide containing 10 mM EDTA, 1.6% SDS, and 0.02% xylene cyanol blue. An aliquot was loaded on a 7% polyacrylamide sequencing gel.

RESULTS

Putative YncC targets revealed by ProteinChip SELDI-TOF analyses—In a search for genes regulated by σ^S in *S. Typhimurium*, we isolated a transposon insertion in the *yncC* gene (7, ATCC-F12) (Table I). SELDI-TOF ProteinChip technology was used to capture and analyze proteins from clear lysates of the wild-type strain ATCC14028 and its mutant derivative ATCC-F12 grown to stationary phase in LB at 37 °C. When spectra from ATCC14028 and ATCC-F12 were compared, three peaks were reproducibly detected with a higher intensity in ATCC14028 than in ATCC-F12 (peaks 1–3, data not shown). Mutant ATCC Δ *yncC*, which contains a deletion of the *yncC* gene, was subsequently constructed (Table I) and compared with ATCC14028. The three peaks, (1, 2, and 3 of molecular sizes 18,641, 18,964, and 31,935 Da, respectively, Fig. 1A) were detected at higher intensity levels in ATCC14028 than in ATCC Δ *yncC* (*p* value 0.004, 6 samples per strain as described under “Experimental Procedures”). Interestingly, these peaks were not detected at significant levels in the spectra of the Δ *rpoS* mutant of ATCC14028 (ATCC Δ *rpoS*, Fig. 1A). Therefore, these peaks might correspond to proteins encoded by genes regulated by σ^S and YncC.

Identification of YncC Targets—Because peak 3 was detected in the wild-type extract with a low intensity, compared with the other two peaks (Fig. 1A), we first focused on the identification of peaks 1 and 2. To identify these proteins, a partial purification scheme was devised (Experimental Procedures) involving anion exchange chromatography of clear lysates from the wild-type strain and the *rpoS* and *yncC* mu-

tants followed by separation on the basis of pI. In the pH 5 fraction, two bands corresponding to proteins of 20 and 17 kDa were detected at a higher intensity in the extract of the wild-type strain than in the *yncC* and *rpoS* mutant extracts (Fig. 1B, lanes 3, 5, and 6). The two bands (shown by stars on Fig. 1B) were cut from the gel for subsequent trypsin digestion and identification by mass spectrometry (Table III) (Experimental Procedures). The proteins were identified as the YciF and YciE proteins of *Salmonella* (Fig. 1B).

The YciF and YciE proteins are encoded by an operon, *yciGFEkatN* (12) (Fig. 1C). Their calculated molecular sizes (Fig. 1C) correspond to those predicted from SELDI-TOF. The elution of these proteins from the anion exchange resin at pH 5 (Fig. 1B) is consistent with the calculated pI of YciF (5.24) and YciE (5.14). In addition, the 20 and 17 kDa proteins were not detected in ATCC-F1, which has a polar transposon insertion in *yciF* (Fig. 1B, lane 4).

The last gene in the operon, *katN*, encodes a protein of 31,848 Da that might correspond to peak 3 detected by SELDI-TOF (Fig. 1A). To check that peaks 1, 2, and 3 are encoded by the *yciGFEkatN* locus, the proteome of strain ATCC Δ *yci*, in which the entire *yciGFEkatN* operon is missing (Table I), was compared with that of the wild-type strain. The spectra of the two strains were similar, except that peaks 1, 2, and 3 were not detected in ATCC Δ *yci* (Fig. 1A), indicating that these peaks corresponded to YciF, YciE, and KatN. Peak 3, corresponding to KatN, has a molecular size (31,935 Da) that is slightly higher than that expected (31,848 Da). This difference might result from the presence of manganese in KatN (12) or from unknown posttranslational modification(s).

The relative abundance of the three proteins (YciF > YciE > KatN, Fig. 1A), is consistent with the position of the genes in the *yciGFEkatN* operon and mRNA levels (12). These proteins were not detected at significant levels in the Δ *rpoS* mutant, in agreement with our previous finding that expression of the operon is highly dependent on σ^S (12, 21). The YciG protein (6 kDa), encoded by the operon, was not detected, likely because conditions used for SELDI-TOF analyses were optimized for accurate detection of proteins > 10 kDa and because the calculated pI of YciG (9.99) is too high for it to bind to the anion exchange array.

YncC is Required for Maximal Transcription of the *yciGFEkatN* Operon in *Salmonella*—Results described earlier indicate that YciF, YciE, and KatN production is positively regulated by YncC. To determine whether this regulation operates at the transcriptional level, kinetics of expression of a *katN-lacZ* gene fusion in the wild-type strain and the Δ *yncC* mutant were compared. Expression of the fusion was delayed during early growth stages and was reduced by the Δ *yncC* mutation (Fig. 2A). The *yncC* gene in pACK Δ *yncC* complemented the Δ *yncC* mutation for *katN-lacZ* expression, confirming that *yncC* activates *katN* transcription (Fig. 2B). In the wild-type strain, expression of *katN-lacZ* was induced earlier during growth and its expression level increased when *yncC* was ex-

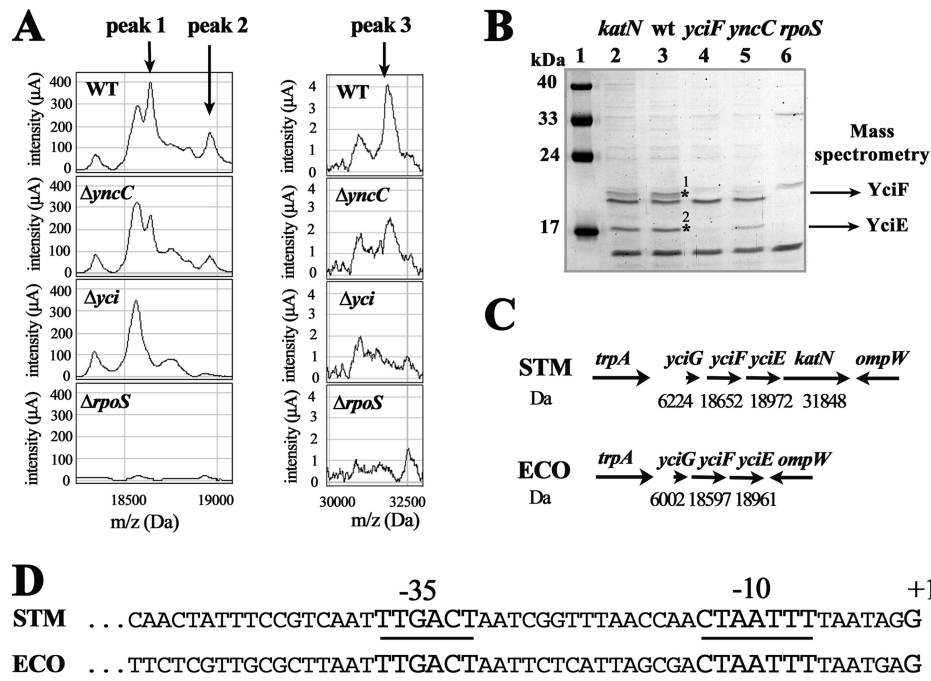


FIG. 1. Identification of protein targets for YncC regulation in *Salmonella*. **A**, Selective capture of proteins from cell lysates of *S. Typhimurium* wild-type and mutant strains onto Q10 ProteinChip Array. Clear lysates from ATCC14028 (WT) and its mutant derivatives ATCC $\Delta yncC$, ATCC $\Delta rpoS$ and ATCC Δyci were applied to the surface of a Q10 ProteinChip as described in the Experimental Procedures section. The captured proteins were detected using surface enhanced laser desorption/ionization (SELDI) time-of-flight mass spectrometry. The normalized mass (m/z) for each peak (in Da) is demonstrated on the x-axis, whereas intensity (μA) is plotted on the y-axis. Extracts were examined several times at different laser energies, and energies of 4500 nJ and 3200 nJ were found to be optimal for detection of peaks 1, 2, and peak 3, respectively. To pick out peak 3, the first pass peak detection was performed with a s/n threshold of two instead of five (Experimental Procedures). The relevant portion of the spectra from a representative experiment is shown. Similar results were obtained in two other experiments. The arrows indicate proteins expressed at different levels in the wild-type and the mutant strains. **B**, Partial purification of proteins of interest for identification by mass spectrometry. The pH 5 fraction (25 μl) of the Q Ceramic HYPERD F exchange resin from lysates of 2: ATCC $\Delta katN-lacZ$, 3: ATCC14028; 4: ATCC-F1; 5: ATCC-F12; and 6: ATCC $\Delta rpoS$ were loaded on the gel. 1: molecular weight markers (in kDa). The stars indicate the protein bands that were excised from the gel and identified as the YciF and YciE proteins by mass spectrometry. **C**, Schematic representation of the *yciGFE(katN)* loci in *Salmonella* (STM) and *E. coli* K-12 (ECO). The molecular sizes of the gene products are indicated in Daltons (Da). **D**, The *yciG* promoters in *Salmonella* and *E. coli* K-12. The relevant portion of the sequence in *Salmonella* ATCC14028 (STM) and *E. coli* MG1655 (ECO) is shown.

TABLE III
Protein identifications

Band ^a	Protein name	Accession number ^b	Matched/ searched ^c	Sequence coverage %	Mascot Protein Score	Protein Confidence Index %	Sequence confirmed by CID ^c	Mascot Ion Score
1	YciF	gi16760152	5/21	37	247	100	⁵⁸ IDQIVESESGIK ⁶⁹ ⁴⁰ LSQAFQSHLEETQGQIER ⁵⁷	83 128
2	YciE	gi16760151	7/17	51	191	100	¹⁴⁷ HIPQTTEQFLLR ¹⁵⁸ ¹ MNYTEHYHDWLR ¹²	73 42

^a Bands are shown in Fig. 1B.

^b Genbank accession numbers for protein sequences 100% identical to that in *Salmonella* strain ATCC14028 (predicted from the nucleotide sequence of the genome, 29).

^c Detailed data are shown in Tables 4 and 5 (supplementary data).

pressed *in trans* from pACK $\Delta yncC$, suggesting that YncC might be a limiting factor for *katN-lacZ* expression under these conditions (Fig. 2B). As expected (12), *katN-lacZ* was expressed at very low levels in the absence of σ^S (Fig. 2F, lanes 1 and 2). Neither the $\Delta yncC$ mutation nor pACK $\Delta yncC$ had any effect on the expression of *lacZ* fused to *katE*, a

catalase encoding gene also regulated by σ^S and used as a control (data not shown). Altogether, these results suggest that YncC exerts a positive effect on *yciGFEkatN* operon transcription.

YncC Binds Upstream of the yciGFEkatN Promoter—Plasmid p $\Delta yncC_{HIS}$ encodes a recombinant YncC protein contain-

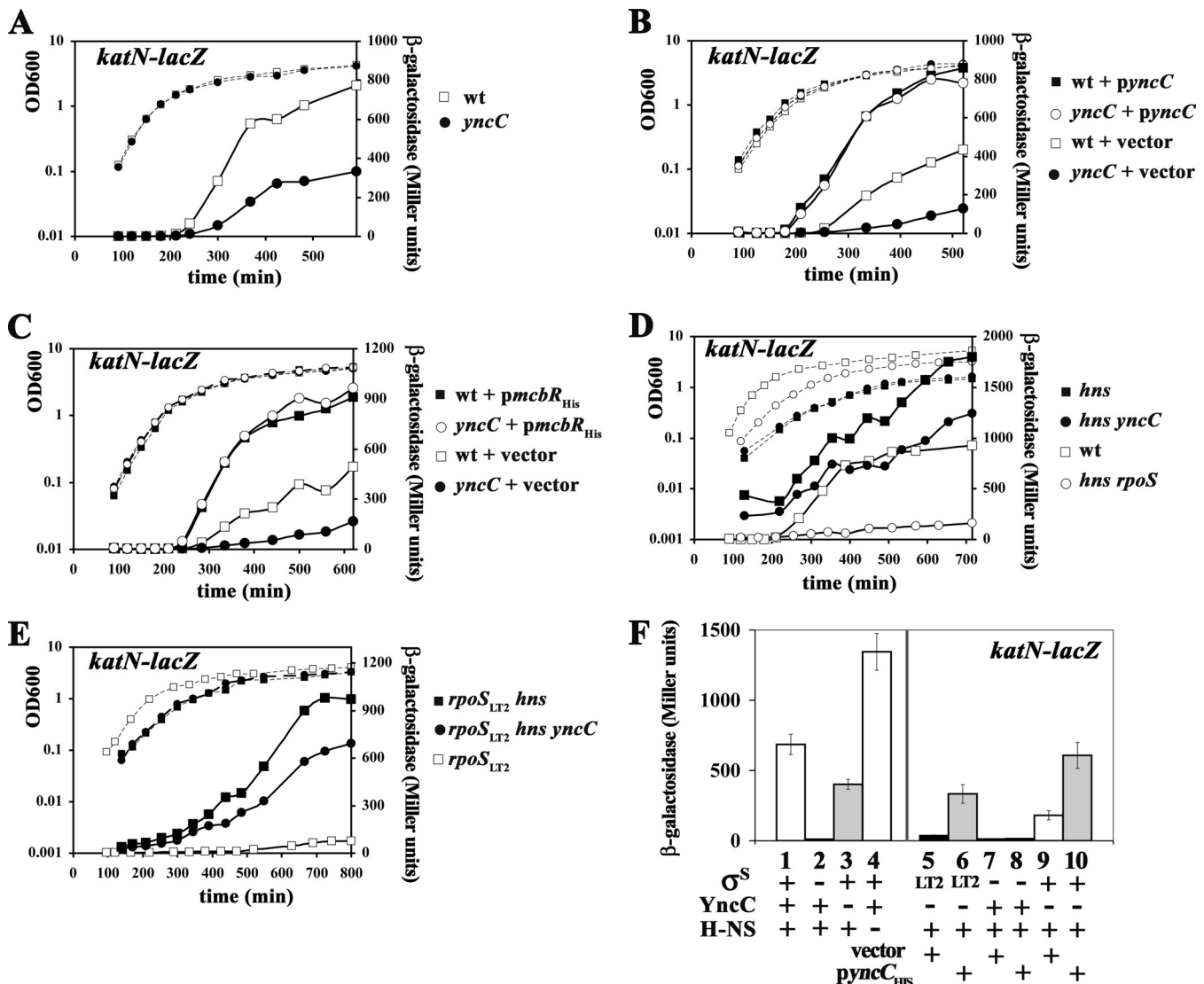


FIG. 2. Expression of a *katN-lacZ* fusion in *Salmonella* wild-type and mutant strains. A–E, Kinetics of *katN-lacZ* expression relative to growth phase. *Salmonella* strains were grown in LB at 37 °C. Exponential-phase cultures (optical density at 600 nm = 0.5) were diluted into LB pre-warmed at 37 °C to prolong the exponential phase. Aliquots were removed at various time intervals and β -galactosidase activity measured (lines) according to the method of Miller (32). The growth phase was determined by measuring the culture turbidity at an optical density of 600 nm (dashed lines). The measurements were repeated at least twice, and a representative experiment is shown. A, ATCC *katN-lacZ* and ATCC *yncC katN-lacZ*. B, ATCC *katN-lacZ* and ATCC *yncC katN-lacZ* containing pACK (vector) and pACK*yncC* (*pyncC*). C, ATCC *katN-lacZ* and ATCC *yncC katN-lacZ* containing pCABg (vector) and *pmcbR*_{HIS}. D, ATCC *katN-lacZ*, ATCC *hns katN-lacZ*, ATCC *hns rpoS katN-lacZ* and ATCC *hns yncC katN-lacZ*. E, ATCC *rpoS*_{LT2} *katN-lacZ*, ATCC *rpoS*_{LT2} *hns katN-lacZ* and ATCC *rpoS*_{LT2} *hns yncC katN-lacZ*. F, Expression of the *katN-lacZ* fusion in the *Salmonella* strains indicated was determined in overnight LB cultures at 37 °C. 1, ATCC *katN-lacZ*; 2, ATCC *rpoS katN-lacZ*; 3, ATCC *yncC katN-lacZ*; 4, ATCC *hns katN-lacZ*; 5, ATCC *rpoS*_{LT2} *yncC katN-lacZ* (pQE30); 6, ATCC *rpoS*_{LT2} *yncC katN-lacZ* (*pyncC*_{HIS}); 7, ATCC *rpoS katN-lacZ* (pQE30); 8, ATCC *rpoS katN-lacZ* (*pyncC*_{HIS}); 9, ATCC2922 *yncC katN-lacZ* (pQE30); 10, ATCC2922 *yncC katN-lacZ* (*pyncC*_{HIS}).

ing six histidine residues at its N terminus (His₆-YncC), under the control of the IPTG-inducible promoter of pQE30. *pyncC*_{HIS}, but not the pQE30 vector, complemented the Δ *yncC* strain for *katN-lacZ* expression and increased *katN-lacZ* expression in the wild-type strain (Fig. 2F, lanes 9 and 10 and data not shown), indicating that His₆-YncC is active. The recombinant protein was over-produced in *E. coli*, purified and used for DNase I footprinting experiments on both

strands of the *Salmonella yciG* promoter region (*yciG*_{STM}) (Fig. 3). His₆-YncC protected a 24 bp sequence centered on the –100 region (Fig. 3B) relative to the transcription start site (14). The YncC binding site is AT-rich and contains the inverted repeat AATATAT. As expected, a footprint was not detected in the *katE* upstream promoter region (data not shown).

YncC also Binds to the E. coli K-12 yciGFE Promoter Region—The ortholog of *yncC* in *E. coli* K-12 (named *mcbR*),

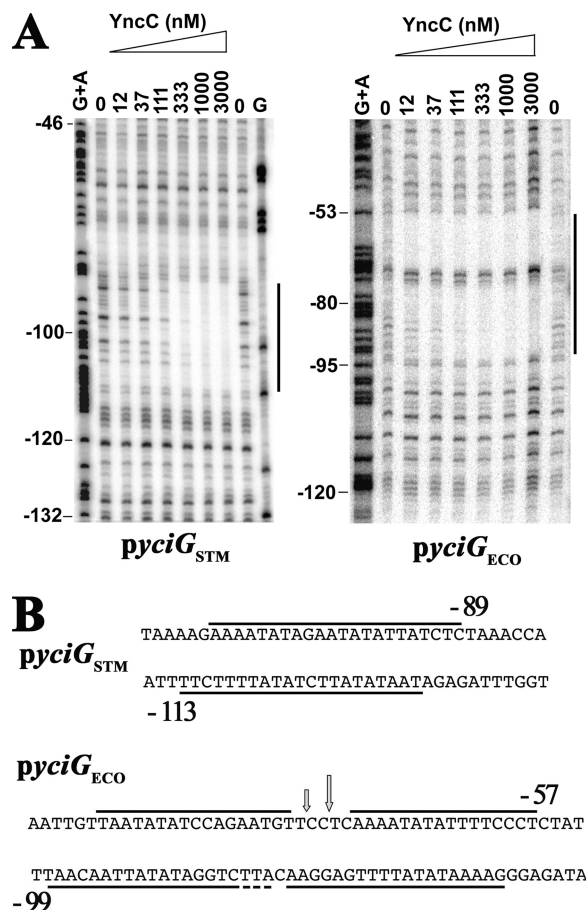


FIG. 3. DNase I footprinting analysis of YncC binding at the *pyciG*_{STM} and *pyciG*_{ECO} promoter regions. **A**, The 5'-radiolabeled DNA fragments (nontemplate strands) were incubated at 37 °C for 20 min with increasing concentrations of His₆-YncC (indicated above each lane) and subsequently treated with DNase I. All samples were analyzed on a denaturing 7.5% polyacrylamide gel. The black lines indicate the regions protected from DNase I cleavage by His₆-YncC. The first lanes correspond to the A + G Maxam and Gilbert sequencing reaction of the probe used as size marker and the nucleotide positions with respect to the *yciG* transcription start sites are indicated on the left. The last lane of the *pyciG*_{STM} autoradiogram corresponds to the G sequencing reaction. **B**, Sequences of the YncC binding sites. The nucleotide sequences of the protected regions are underlined on both nontemplate and template strands. The borders of the protected regions are marked with respect to the transcription start site.

regulates colanic acid production by repressing expression of the *ybiM* gene (13). Deletion of *mcbR* in *E. coli* MG1655 elicited mucoidy and decreased biofilm formation because of overproduction of colanic acid (13). The *yncC* mutants of *Salmonella*, ATCC-F12 and ATCC*yncC*, were not mucoid (data not shown), consistent with the absence of *ybiM* from *S. Typhimurium* genome (<http://www.ncbi.nlm.nih.gov/>).

In both *Salmonella* and *E. coli* K-12, *yncC/mcbR* is located between the *yncB* and *yncD* genes that encode a putative oxidoreductase and a putative iron outer membrane transporter, respectively. However, the intergenic regions between

yncB and either *yncC* in *Salmonella* or *mcbR* in *E. coli* K-12 MG1655, which likely contain the *yncC/mcbR* promoter, differ in length and sequence, suggesting that *yncC* and *mcbR* might be differentially regulated. In addition, the amino acid sequences of YncC and McbR diverge in the C-terminal domain (46% identity over amino acids 78 to 221), compared with the N-terminal domain (81% identity over amino acids 1 to 77), which contains the predicted DNA binding HTH domain (8, 9). The C terminus of regulators of the GntR/FadR family contains an effector-binding and/or oligomerisation domain that influences the DNA-binding properties of the regulator (8–10). Altogether, these findings suggested that YncC and McbR might have evolved to respond to different signals and/or perform different functions in *E. coli* K-12 and *Salmonella*.

The *yciGFE* locus is conserved in *E. coli* K-12, but *katN* is not (Fig. 1C). The –35 and –10 elements of the *yciGFEkatN* promoter in *Salmonella* (*pyciG*_{STM}, 12) are conserved in *E. coli* K-12 (Fig. 1D). However, the DNA region upstream of the –35 element, including the YncC binding site identified upstream of *pyciG*_{STM}, diverge in the two species. Nevertheless, the His₆-YncC protein could bind to the *yciG*_{ECO} promoter region (*pyciG*_{ECO}) (Fig. 3). The footprint containing two repeats of the AATATAT motif extended over 42 bp with two hypersensitive bands located on the nontemplate strand at the center of the protected region.

YncC belongs to the GntR subfamily of FadR (pfam007729), which binds as a dimer to its operator site via its winged helix domains (10). In the x-ray structure of the FadR-operator complex, the two recognition helices of each monomer project into a central major groove and the two β ribbons of the wings into the flanking minor grooves resulting in specific DNA-protein interactions over 11 bp. Based on these data, YncC likely binds DNA as a dimer and we predict that at least two tandem YncC operator sites are present upstream of the *pyciG*_{ECO} promoter. The protection footprint of about 20 bp at *pyciG*_{STM} suggests the presence of a single YncC binding site. Interestingly the YncC binding sites are located closer to the transcription start site at *pyciG*_{ECO} than at *pyciG*_{STM} (Fig. 3B).

The *E. coli* K-12 His₆-McbR protein and the *Salmonella* His₆-YncC protein showed similar protection footprint patterns at the *pyciG*_{STM} and *pyciG*_{ECO} promoters (data not shown), a finding consistent with the high sequence conservation in the DNA binding domains of these proteins.

The yciGFE Locus is Poorly Expressed in E. coli K-12—To determine the functional relevance of YncC/McbR binding to the *yciGFE* promoter region in *E. coli* K-12, the ability of *E. coli* MG1655 wild-type strain and mutant derivatives to produce the YciF and YciE proteins was assessed by SELDI-TOF technology. However, the spectra obtained for the wild-type strain and the $\Delta yciF$ and $\Delta yciE$ mutants were similar (data not shown) and peaks corresponding to YciF and YciE could not be detected (Fig. 4A). To assess the expression of these

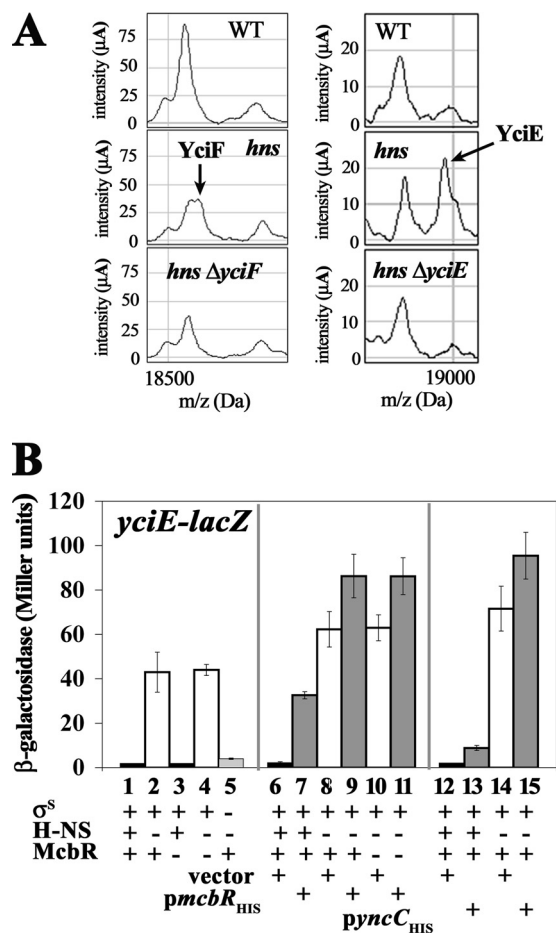


FIG. 4. Expression of the *yciGFE* locus in *E. coli* K-12 strains. A, SELDI-TOF-MS profiles of *E. coli* MG1655 and its mutant derivatives using the Q10 ProteinChip array. Clear lysates from MG1655 (WT) and its mutants MG655*hns*, MG1655*hnsyciE*, and MG1655*hnsyciF* were applied to the surface of a Q10 ProteinChip as described in the Experimental Procedures section. The captured proteins were detected using surface enhanced laser desorption/ionization (SELDI) time-of-flight mass spectrometry. Normalized mass (*m/z*) for each peak (in Daltons (Da)) is demonstrated on the *x*-axis, whereas intensity (μ A) is plotted on the *y*-axis. A laser energy of 3200 nJ was used. The relevant portion of the spectra is shown. The arrows indicate the YciE and YciF proteins. B, Expression of the *yciE-lacZ* fusion in the *E. coli* strains indicated was determined in overnight LB cultures at 37 °C. Lanes 1 to 5: (1) MC4100 *yciE-lacZ*, (2) MC4100*hns yciE-lacZ*, (3) MC4100*mcbR yciE-lacZ*, (4) MC4100*hnsmcbR yciE-lacZ*, (5) MC4100*hnsrpoS yciE-lacZ*. Lanes 6 to 15: MC4100 *yciE-lacZ* harboring pCABg (6), *pmcbR*_{HIS} (7), pQE30 (12), and *pyncC*_{HIS} (13); MC4100*hns yciE-lacZ* harboring pCABg (8), *pmcbR*_{HIS} (9), pQE30 (14), and *pyncC*_{HIS} (15); and MC4100*hnsmcbR yciE-lacZ* harboring pCABg (10), and *pmcbR*_{HIS} (11).

genes in *E. coli* K-12 further, a chromosomal *yciE-lacZ* transcriptional fusion was constructed in two *E. coli* K-12 Lac⁻ strains, MC4100 and MC1061. The fusion was expressed at very low levels in both strains and in their Δ *mcbR* and Δ *rpoS* mutant derivatives (Fig. 4B, lane 1 and data not shown). The His₆-McbR and His₆-YncC proteins were able to induce *yciE-lacZ* expression, although the levels of expression remained

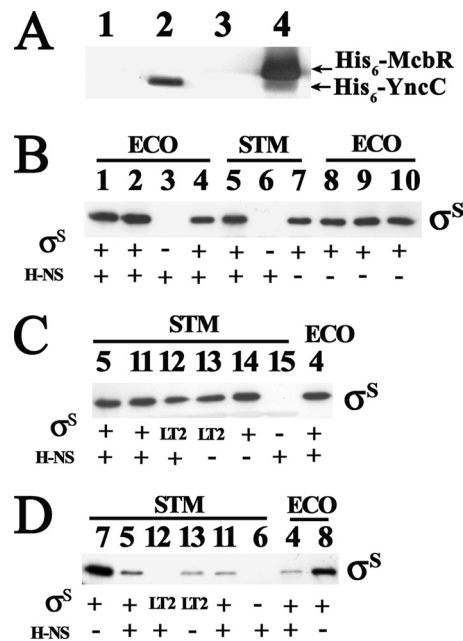


FIG. 5. Immunodetection of σ^S , His₆-YncC and His₆-McbR. A) Detection of His₆-McbR and His₆-YncC produced from *pmcbR*_{HIS} and *pyncC*_{HIS}, respectively. *E. coli* strains, harboring *pyncC*_{HIS}, *pmcbR*_{HIS} and the vectors pACBg and pQE30, were grown to stationary phase in LB at 37 °C and analyzed by Western blotting with anti-His antibodies. A 5- μ g aliquot of total protein was loaded in each slot. 1: MC4100 *yciE-lacZ* (pQE30), 2: MC4100 *yciE-lacZ* (*pyncC*_{HIS}), 3: MC4100 *yciE-lacZ* (pCABg), 4: MC4100 *yciE-lacZ* (*pmcbR*_{HIS}). Compared with the wild-type YncC/McbR proteins, the His₆-McbR and His₆-YncC proteins contain 18 and 10 additional amino acids; thus, His₆-McbR migrates more slowly on SDS-PAGE than the His₆-YncC protein. B–D, Detection of σ^S in *Salmonella* (STM) and *E. coli* K-12 (ECO) strains in exponential phase (D) or stationary phase (B, C) in LB at 37 °C were analyzed by Western blotting with anti- σ^S antibodies. 10 μ g of total protein was loaded in each slot. 1: MC1061, 2: MG1655, 3: MC4100*rpoS*, 4: MC4100, 5: ATCC14028, 6: ATCC*rpoS*, 7: ATCC*hns*, 8: MC4100*hns*, 9: MG1655*hns*, 10: MC1061*hns*, 11: ATCC2922K, 12: ATCC*rpoS*_{LT2}, 13: ATCC*rpoS*_{LT2}*hns*, 14: ATCC2922K*hns*, 15: ATCC2922K*rpoS*.

low (Fig. 4B, lanes 6 and 7 and 12 and 13, respectively). *yciE-lacZ* expression was induced to higher levels by His₆-McbR than by His₆-YncC (Fig. 4B, lanes 7 and 13), likely because the former is more abundant (Fig. 5A). Like the His₆-YncC protein, the His₆-McbR protein activated expression of the *katN-lacZ* fusion in the Δ *yncC* and wild-type strains of *Salmonella* (Fig. 2C). Altogether, these results show that YncC and McbR are both able to induce expression of the *yciGFE(katN)* locus in *Salmonella* and *E. coli* K-12, and that this locus is expressed at drastically lower levels in *E. coli* K-12 than in *Salmonella*.

Gene Polymorphism at the *trpA-yciGFE-ompW* Locus in *E. coli* Strains—The low GC content of the *yciF* and *yciE* genes relative to the resident genome suggested that these genes were horizontally acquired in *E. coli* K-12 (38) and *Salmonella* (39, 40). Interestingly, in nearly half of the 23 complete sequenced genomes of *E. coli* strains (<http://www.>

ncbi.nlm.nih.gov/), the *trpA-yciGFE-ompW* locus (Fig. 1C) is a site of DNA rearrangements, including deletions and/or insertions of phage related—and/or virulence associated—genes. In addition, in pathogenic *E. coli* O157:H7, a second copy of the *yciGFE* locus, including the *katN* gene, is located on a cryptic prophage (CP-933X) elsewhere in the genome. The sequence identity between the prophage-borne gene products in *E. coli* O157:H7 and corresponding gene products in *E. coli* K-12 and *Salmonella* is high (more than 80%). However, the noncoding sequence upstream of the prophage-borne *yciGFEkatN* genes is different from those upstream of *yciG_{ECO}* and *yciG_{STM}* and does not contain the -10 and -35 promoter elements present in the two other loci (data not shown). The *yciGFEkatN* genes are absent from the closest *E. coli* relative, *E. fergusonii* (<http://www.ncbi.nlm.nih.gov/>). Altogether, these findings are consistent with horizontal acquisition of these genes in *E. coli*.

In contrast to the situation in *E. coli*, the *yciGFEkatN* locus belongs to the core genome in *Salmonella* (41), suggesting that *Salmonella* acquired these genes before the lineage divided into the two *Salmonella* species, *S. enterica* and *S. bongori*. The 479 pb sequence between *trpA* and *yciG* (Fig. 1C) is also conserved in the 16 complete sequenced genomes of *S. enterica* (<http://www.ncbi.nlm.nih.gov/>) and in *S. bongori* (<http://www.sanger.ac.uk/Projects/Salmonella/>). The sequence of the -10 and -35 elements is identical in all these *Salmonella* genomes. The sequence of the YncC binding region (in *pyciG_{STM}*) (Fig. 3B) is 100% identical in the genomes of *S. enterica* subsp. *enterica* and only one mismatch is found at the boundaries of this motif (Fig. 3B) in the two most ancestral groups (41), *S. enterica* subsp. *arizonae* (T/C at position -91) and *S. bongori* (G/A at position -110).

H-NS Silencing of yciGFEkatN is Relieved in Stationary Phase by σ^S in Salmonella—H-NS is an abundant histone-like protein that binds preferentially to AT-rich DNA and subsequently oligomerizes along the DNA resulting in the formation of extended nucleoprotein complexes that cause gene repression (14–16). Preferential binding of H-NS to sequences with higher AT-content than the resident genome allows H-NS to repress the expression of foreign DNA in a process known as “xenogeneic silencing” (15, 16). Selective silencing of foreign DNA with low GC content in *Salmonella* by H-NS has been reported using chromatin immunoprecipitation and microarray analyses (39, 40). Examination of these data revealed that H-NS binds the *yciGFEkatN* locus and represses its expression.

In agreement with these findings, expression of *katN-lacZ* in *S. Typhimurium* ATCC14028 (Fig. 2D) and SL1344 (data not shown) was increased by an *hns* mutation by more than 10-fold in exponential phase and by twofold in stationary phase. In the *hns* mutants, σ^S was still required for *katN-lacZ* expression (Fig. 2D and data not shown). The growth rate of *Salmonella* was highly affected by the *hns* mutation (Fig. 2D). H-NS is required for the normal proteolytic turnover of σ^S (42)

and, thus, levels of σ^S in the exponential phase were higher in the *hns* strains than in the wild-type strains (Fig. 5D, lanes 5 and 7). As previously reported (39, 40), the high σ^S content in the *hns* strain likely impairs growth, because the growth defect of the *hns* mutant can be partially alleviated by deleting *rpoS* (Fig. 2D) or by replacing the wild-type *rpoS* allele by the *rpoS_{LT2}* allele (Fig. 2E). The *rpoS_{LT2}* allele contains a rare TTG start codon (instead of ATG). This mutation lowered the σ^S level in ATCC*rpoS_{LT2}* and ATCC*rpoS_{LT2}hns* in exponential phase (Fig. 5D, lanes 5, 7, and 11, and lanes 7 and 13) and to a lesser extent in stationary phase (21) (Fig. 5C, lanes 5 and 11–14). In stationary phase, derepression of *katN-lacZ* expression by the *hns* mutation was stronger in ATCC*rpoS_{LT2}* than in ATCC14028 (12- and twofold respectively, Figs. 2D, E). However, σ^S levels and *katN-lacZ* expression levels in stationary phase were not highly different in the two *hns* strains (twofold difference) (Figs. 2D, E and Fig. 5C lanes 13 and 14). These results suggested that the reduction in σ^S level, because of the *rpoS_{LT2}* mutation, potentiated the magnitude of repression of *katN-lacZ* expression by H-NS.

σ^S is not Efficient to Counter H-NS Silencing of yciGFE in E. coli K-12—Two peaks of 18,590 and 18,961 Da, likely corresponding to the YciF and YciE proteins, were detected by SELDI-TOF ProteinChip analyses in the Δhns mutant of MG1655 but not in the $\Delta hns\Delta yciF$ and $\Delta hns\Delta yciE$ mutants respectively (Fig. 4A). Detection of the YciE and YciF proteins in the *hns* mutant but not in the wild-type strain (Fig. 4A) suggested that expression of these proteins is silenced by H-NS in *E. coli* K-12, in agreement with a previous finding (43). Expression of the *yciE-lacZ* fusion was consistently derepressed in the *hns* mutant of MC4100 (Fig. 4B, lanes 1 and 2). Expression of the *yciE-lacZ* fusion in the *hns* strain was strongly affected by the *rpoS* mutation (Fig. 4B, lanes 2 and 5). These results indicated that σ^S induces expression of *yciGFE* in *E. coli* K-12 only when H-NS mediated repression was relieved. Repression of *yciGFE(katN)* by H-NS is inversely correlated with the σ^S levels (Figs. 2D, E and Figs. 5C, D), and, thus, one possible explanation for these results is that *E. coli* produces less σ^S than *Salmonella*. This hypothesis was ruled out because similar levels of σ^S were detected in MG1655, MC4100, MC1061, and ATCC14028 (Figs. 5B, C, D). In addition, similar levels of σ^S were detected in the *hns* derivatives of these strains (Fig. 5B and data not shown).

YncC Directly Activates $E\sigma^S$ -dependent In Vitro Transcription at pyciG_{STM}—Significant expression of the *yciGFEkatN* operon was not detected in the $\Delta rpoS$ mutant of *Salmonella* (12) (Fig. 2F, lane 2), and *katN-lacZ* expression was very low in the *rpoShns* strain of *Salmonella* (Figs. 2D, E). These results suggested that *pyciG_{STM}* is not efficiently transcribed in the absence of σ^S . In agreement with this conclusion, a transcript initiating at *pyciG_{STM}* was detected *in vitro* with the $E\sigma^S$ -holoenzyme ($E\sigma^S$) but not with σ^{70} -holoenzyme ($E\sigma^{70}$) (Fig. 6B).

In plasmids pACK*yncC* and *pyncC_{HIS}*, *yncC* lacks its own promoter and is transcribed from the promoters in the vectors

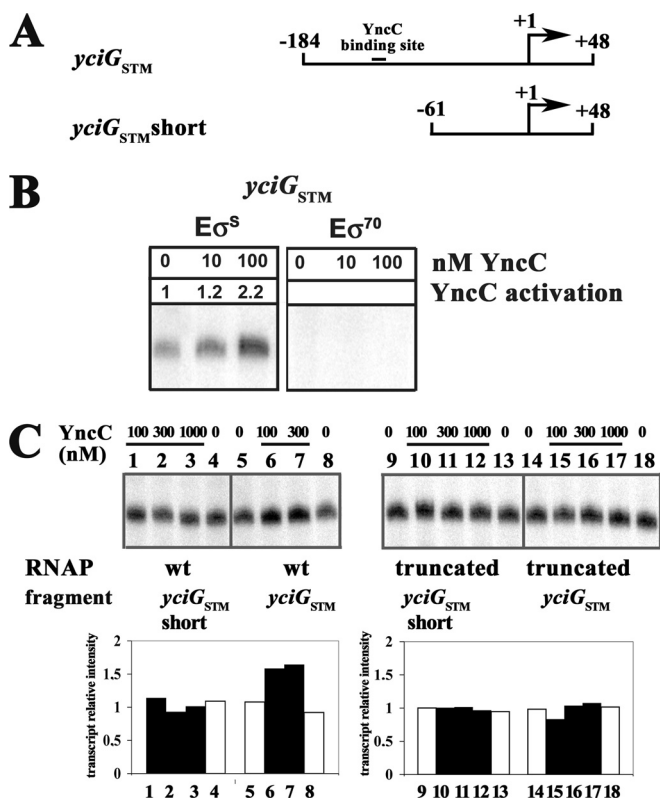


FIG. 6. YncC transcriptional activation at *yciG*_{STM}: requirements for σ^S and the C-terminal domain of the α subunit of RNA polymerase. *A*, long (*yciG*_{STM}) and short (*yciG*_{STM}^{short}) versions of *yciG*_{STM}: the regions inserted upstream of the *rrnB1T1* terminator are indicated with respect to the transcription start site. *B*, Single round run-off transcripts of the *yciG*_{STM} fragment using 15 nM native core RNA polymerase and 60 nM σ^S or σ^{70} following 20 min preincubation with 0, 10, or 100 nM His₆-YncC. *C*, Single round run-off transcripts of *yciG*_{STM}^{short} (lanes 1–4, 9–13) and *yciG*_{STM} (lanes 5–8, 14–18) using native core (lanes 1–8) or α -C-terminal truncated RNA core (lanes 9–18). YncC concentrations were 0 nM (lanes 4, 5, 8, 9, 13, 14, and 18), 100 nM (lanes 1, 6, 10, and 15), 300 nM (lanes 2, 7, 11, and 16), and 1 μ M (lanes 3, 12, and 17). Quantification of the *yciG*_{STM} transcript is provided below each lane.

(Table I). pACK_{YncC} and *pyncC*_{HIS} did not induce expression of *katN-lacZ* in the exponential phase of growth (Fig. 2B and data not shown). In addition, *pyncC*_{HIS} did not induce expression of the fusion in the *rpoS* and *rpoShns* strains (Fig. 2F, lanes 7 and 8 and data not shown). These results suggested that YncC and σ^S act in concert to induce full expression of the operon. Consistent with these findings, YncC induced *in vitro* transcription by $E\sigma^S$, but not by $E\sigma^{70}$, at *yciG*_{STM} (Fig. 6B). YncC activation was moderate (2 ± 0.6 at 100–300 nM YncC) but reproducible in six independent experiments (Figs. 6B, C and data not shown). YncC was without effect when the fragment used for transcription lacked the YncC DNA binding region, (*yciG*_{STM} short) (Figs. 6A, C). YncC was also without effect on transcription initiation at the σ^S -dependent *katE* promoter (Fig. 7) (lanes 17 and 18) in agreement with *in vivo* data (not shown). Interestingly, transcription activation by

YncC was not detected with a RNA polymerase in which the α subunit lacks the C-terminal domain (Fig. 6C). These results suggested that transcription activation by YncC requires the α CTD domain.

*YncC activates transcription at *yciG*_{ECO} by counteracting H-NS-mediated silencing*—The core promoter regions of *yciG*_{ECO} and *yciG*_{STM} are very similar (Fig. 1D) and, as expected, transcription initiation occurred at similar sites *in vitro* (Fig. 7). Like *yciG*_{STM}, *yciG*_{ECO} was selectively transcribed by $E\sigma^S$ (data not shown). However, in contrast to *yciG*_{STM}, *yciG*_{ECO} was not activated by YncC (Fig. 7, lanes 1 and 2 and data not shown). Addition of H-NS strongly decreased transcription by $E\sigma^S$ at *yciG*_{ECO} (5- to 100-fold) (Fig. 7, lanes 1, 3, 5, and 7), as expected from *in vivo* data (Fig. 4). YncC decreased the magnitude of H-NS-mediated repression (Fig. 7, lanes 3–8). The *katE* promoter, used as a control, was hardly repressed by H-NS and was insensitive to YncC (Fig. 7, lanes 17–24), in agreement with *in vivo* data (not shown). These results suggested that activation of *yciE-lacZ* expression in *E. coli* by His₆-McbR and His₆-YncC (Fig. 4B) was because of the ability of these proteins to counter H-NS-mediated silencing at *yciG*_{ECO}. Consistent with this hypothesis, YncC/McbR did not have a marked effect on *yciGFE* expression in *E. coli* K-12 in the absence of H-NS (Fig. 4B, lanes 2 and 4, lanes 6–11 and lanes 12–15).

On binding to high affinity “nucleation” sites, H-NS spreads along the DNA to lower affinity sites to occupy the promoter region, allowing the formation of higher order structures. An H-NS binding region contains several sites with variable affinity, and the number and the organization of binding sites determines the formation of a repressive nucleoprotein complex and modulates H-NS repression of gene expression (14–16). DNase I footprinting experiments showed that H-NS binds to the *yciG*_{ECO} promoter region (Fig. 8, lanes 2–5). The binding pattern was marked by a series of protected and hypersensitive bands, indicating that H-NS changes the local topology of the promoter region. The polymerization of H-NS molecules along the promoter sequence would be expected to repress *yciGFE* expression by promoter occlusion or by antagonizing open complex formation. According to the 10-bp consensus binding sequence reported for H-NS nucleation sites (44), two predicted H-NS binding sites of high affinity are located in the upstream promoter region, precisely in the motifs recognized by YncC/McbR. The first site, located in the upstream YncC box AATaTATcCa (Fig. 3B), matches the consensus over 8 bp, whereas the other, AATaTATttt in the downstream YncC box (Fig. 3B), has 6 bp matches and, therefore, is expected to have lower affinity (note that the bases matching the H-NS consensus site are indicated in capital letters).

Many DNA-binding proteins can counter H-NS-mediated silencing, usually through competition for H-NS binding (15, 45). DNase I footprinting experiments with both H-NS and YncC showed that they compete for DNA binding (Fig. 8,

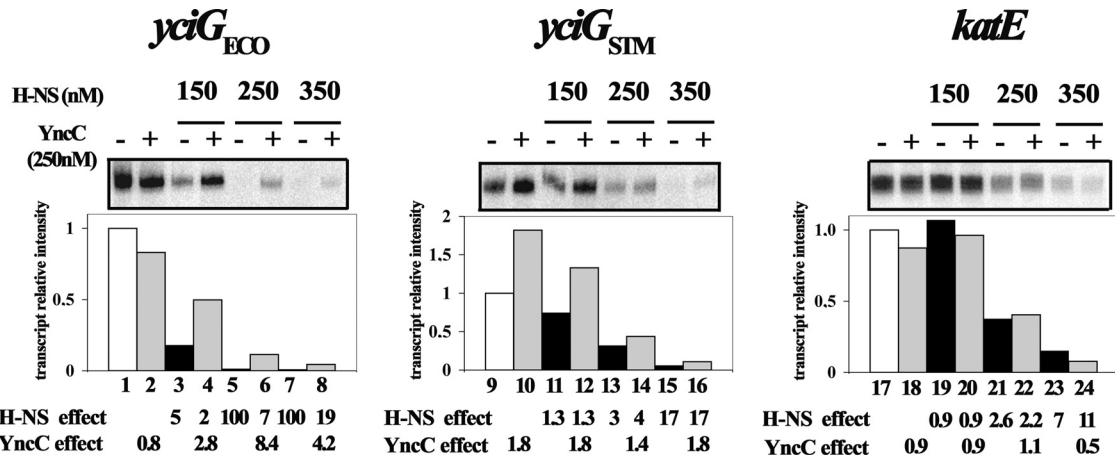


FIG. 7. **Differential effects of YncC on H-NS-mediated repression.** Single round run-off transcripts using DNA fragments containing the promoter regions of *yciG_{STM}* (−184 to +48), *yciG_{ECO}* (−227 to +66) and *katE* (−106 to +66). The templates were first incubated with or without H-NS for 20 min: lanes 1, 2, 9, 10, 17, and 18; no H-NS; lanes 3, 4, 11, 12, 19, and 20, 150 nM H-NS; lanes 5, 6, 13, 14, 21, and 22, 250 nM H-NS; lanes 7, 8, 15, 16, 23, and 24, 350 nM H-NS. The σ^S -RNA polymerase (E: 30 nM; σ^S : 120 nM) was added alone or in combination with YncC (250 nM) and incubation was prolonged for 10 min before addition of the heparin/XTP mixture. The histograms and number below each lane show the quantification of the transcripts and the effects of H-NS and YncC.

lanes 8, 9, and 10). YncC prevented H-NS binding only at high concentrations (Fig. 8, compare lanes 10 and 11). These results suggested that, when present in high amounts in *E. coli*, YncC/McbR counters H-NS mediated-repression at *yciG_{ECO}* (Fig. 4B) by modulating H-NS binding and, ultimately, by counteracting the negative effects of H-NS.

Interplay Between H-NS and YncC at the *yciG_{STM}* Promoter—*In vitro* repression by H-NS was less marked at *yciG_{STM}* than at *yciG_{ECO}* (Fig. 7), a result consistent with *in vivo* data (Figs. 2F and 4B). The magnitude of H-NS repression was not affected by YncC (Fig. 7), and the magnitude of YncC activation was not affected by H-NS (Fig. 7). H-NS was able to bind to *yciG_{STM}*, protecting multiple sites along the DNA leading to the formation of a repression complex (Fig. 8, lanes 12 to 16). As for the *yciG_{ECO}*, two predicted H-NS binding sites (agaATAtATT centered at −98.5 and AtaTTATCTc centered at −93.5) in *yciG_{STM}* overlap the single YncC binding site (Fig. 3B). In the competitive footprinting assay between the two proteins, YncC occupied the *yciG_{STM}* site at a lower concentration than at *yciG_{ECO}*, but this did not appear to prevent H-NS binding at other sites along the promoter fragment (Fig. 8, lanes 20–22). Indeed, some bands around −88, which are not protected by YncC or H-NS alone, are protected in the combined footprint, supporting the notion that H-NS and YncC did not compete for binding but rather bound simultaneously to *yciG_{STM}* fragment (Fig. 8, compare lanes 18 and 22). These results are in agreement with the *in vitro* transcription data (Fig. 7), and suggest that YncC activation and H-NS repression occur independently at *yciG_{STM}*.

The effect of the $\Delta yncC$ mutation on *katN-lacZ* expression in *Salmonella* was attenuated in the absence of H-NS (Figs. 2A, D, E). One possible explanation for this result is that the greater abundance of σ^S in the *hns* strain compared with the wild-type

strain (Fig. 5D) reduced the need for YncC in the absence of H-NS. Indeed, the impact of YncC on *katN-lacZ* expression was greatest at the entry to stationary phase (Figs. 2A, B), when σ^S begins to accumulate in the cells (21), suggesting that the impact of YncC might be greatest at low σ^S concentrations. Consistent with this hypothesis, *katN-lacZ* transcription activation by His₆-YncC was higher in the presence of the *rpoS_{LT2}* allele (ninefold) (Fig. 2F lanes 5 and 6) than in the presence of the wild-type *rpoS* allele (3.5-fold) (Fig. 2F lanes 9 and 10).

DISCUSSION

In the present study, a proteomic method using ProteinChip arrays coupled with surface-enhanced laser desorption/ionisation time of flight mass spectrometry (SELDI-TOF-MS) was used for comparative proteomic profiling of cell extracts from *Salmonella* strains. These experiments revealed three proteins, subsequently identified as the *yciF*, *yciE*, and *katN* gene products that were produced in lower amounts in the *yncC* mutant than in the wild-type strain. Gene fusion analyses and *in vitro* transcription and DNase I footprinting experiments demonstrated that YncC controls production of these proteins at the transcriptional level and acts in concert with σ^S . The σ^S also controls expression of *yncC* (7), and thus, *yciGFEkatN* is regulated by a σ^S -dependent feed-forward regulatory loop. This dual role of σ^S in the control of the operon, and the inverse correlation, observed in this study, between the σ^S level and the magnitude of H-NS repression, might account for the strong sensitivity of *yciGFEkatN* expression to σ^S levels and to activation by CrI (21), the σ^S -chaperone that increases σ^S activity.

Like most σ^S -dependent promoters, *yciG_{STM}* had a moderate activity *in vitro*, which was slightly stimulated by binding of YncC to *yciG_{STM}* (Figs. 3, 6, and 8), and required α CTD of

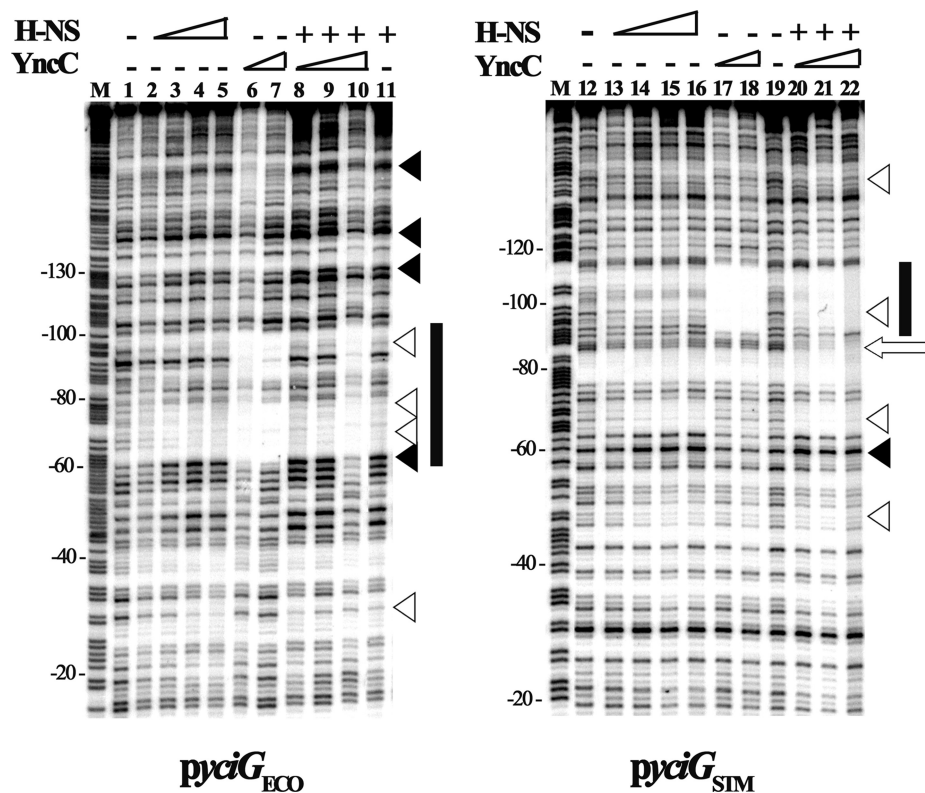


FIG. 8. DNase I footprint analysis of *pyciG_{ECO}* and *pyciG_{STM}* promoters with H-NS, YncC and both proteins. The 5'-radiolabeled promoter fragment (template strand) was incubated with H-NS, YncC or a preformed mixture of both proteins for 20 min before DNase I attack, lanes 1, 12, and 19: no protein; lanes 2 and 13: 37.5 nM H-NS; lanes 3 and 14: 75 nM H-NS; lanes 4 and 15: 150 nM H-NS; lanes 5, 11, and 16: 250 nM H-NS; lanes 6 and 17: 250 nM YncC; lanes 7 and 18: 1 μ M YncC; lanes 8 and 20: 250 nM H-NS with 250 nM YncC; lanes 9 and 21: 250 nM H-NS with 500 nM YncC; lanes 10 and 22: 250 nM H-NS with 1 μ M YncC. M is a Maxam-Gilbert A+G track and the numbering on the left is relative to the transcription start site. Open or black triangles (right side) indicate bands with decreased or enhanced intensity, respectively, in the presence of H-NS. The footprint of YncC is represented to the right by a solid black bar. The location of the bands that are only protected in the presence of both YncC and H-NS is marked with an open arrow.

RNAP (Fig. 6). The results suggested that YncC might act as a class I activator, making direct interactions with α CTD, thereby recruiting the rest of RNA polymerase (46). The location of activator binding in promoters subject to class I activation is variable, because of the flexibility of the linker between the N- and C- terminal domains of the α subunit, but is usually near positions -61 , -71 , -81 or -91 . The position of the YncC binding site, centered at -101 with respect to the transcription start site of *yciG*, is 10 bp upstream of the most distant transcription activators at simple σ^{70} -dependent promoters. However the intrinsic DNA curvature found in many σ^S -regulated promoters (including *pyciG_{STM}*, data not shown) might facilitate protein-protein contacts between YncC and the CTD of the distal α subunit of RNA polymerase, which is used preferentially by $E\sigma^S$ for activation (46–48).

H-NS and YncC can bind DNA simultaneously to regulate *in vitro* transcription at *pyciG_{STM}* (Figs. 7 and 8). *In vivo* however, the magnitude of YncC activation was reduced in the absence of H-NS (Figs. 2D, E). This might result from the high σ^S levels in the *hns* strains, or from the involvement of an additional molecule that regulates *yciGFEkatN* expression. Alternatively,

H-NS not only binds to the promoter region of *yciGFEkatN* (Fig. 8) but also to coding regions (39, 40 and our unpublished results) and might form DNA bridges that contribute to transcription repression (14–16). Significant binding of YncC to the coding sequences tested so far was not observed (data not shown). YncC might help relieve H-NS silencing indirectly, by increasing the transcription initiation rate at *pyciG_{STM}* and, thus, the transcription elongation rate across the H-NS binding region, in line with the situation reported at the *bgl* promoter (49). Further experiments will evaluate the effect of downstream sequences in H-NS silencing of *pyciG_{STM}*.

YncC/McbR and H-NS are also able to bind to the promoter region of the *E. coli* K-12 *yciGFE* genes. However, the sequence, the length, and the position of the McbR/YncC and H-NS binding regions, relative to the *yciGFE(katN)* promoter, are different in *E. coli* K-12 and *Salmonella*, resulting in differential mechanisms of regulation of these genes by YncC/McbR and H-NS. It is remarkable that in *E. coli* K-12, regulation of *yciGFE* by YncC and by H-NS are intimately linked, whereas in *Salmonella*, YncC directly activates transcription, and thus, activation by YncC is, at least partly, disconnected

from the H-NS network. One exciting possibility is that *Salmonella* has evolved the *yciGFEkatN* cis-regulatory sequences to integrate this locus into the RpoS network while maintaining its connection to the H-NS network, ultimately resulting in a more versatile but tightly controlled expression of this locus. The feed-forward regulatory loop mediated by YncC might allow signal input at levels downstream of σ^S itself, through modulation of YncC activity or expression. Our data show that YncC production and/or activity is a limiting factor for *yciGFEkatN* expression and that the impact of YncC is major at low σ^S concentrations. One hypothesis is that YncC induces *yciGFEkatN* expression under a specific environmental condition in the exponential phase of growth where σ^S level is low. Our future experiments will assess environmental signals that might modulate YncC activation of *yciGFEkatN*. These experiments might reveal putative cofactors that bind to the C-terminal domain of YncC and modulate its DNA binding activity.

The evolution of promoter architecture in closely related bacterial species might have important consequences for bacterial adaptation (50–52). The physiological role of the *yciGFE(katN)* locus is unknown, and the significance, in the fitness of *E. coli* and *Salmonella*, of the differential regulation of these genes requires further investigation. Structural comparisons suggest a role for YciF in iron storage and/or protection against oxidative damage (53). KatN belongs to the family of manganese catalases but it does not play a major role in hydrogen peroxide resistance of *Salmonella* under standard growth conditions or in virulence in mice (12, 54). This is because of the functional redundancy of the five hydrogen peroxide scavengers (three catalases and two alkyl hydroperoxide reductases) that contribute to *Salmonella* virulence and oxidative stress resistance (54). Nevertheless, overproduction of KatN increased resistance of *Salmonella* to hydrogen peroxide (12) and enhanced its virulence in NF- κ B pathway mutant *Drosophila* (55), suggesting that KatN might indeed contribute to *Salmonella* fitness. One could speculate on a correlation between gene polymorphism at the *trpA-yciGFE-ompW* locus in *E. coli*, silencing of *yciGFE* by H-NS, and the absence of *katN*. Investigation of the regulation and the role of the prophage-borne *yciGFEkatN* locus in the virulence and fitness of pathogenic *E. coli* O157:H7 strains might provide insight into the evolution and the function of this locus in closely related Enterobacteria.

Acknowledgments—We are grateful to Anthony Pugsley for critical reading of the manuscript, to Pascal Lenormand and Abdelkader Namane (PF3, Institut Pasteur) for mass spectrometry analyses and helpful discussions, to Sylvie Rimsky (ENS-Cachan) for providing the H-NS protein, to Jacqueline Plumbridge (IBPC-Paris) for advice and helpful discussions, and to the National BioResource Project (National Institute of Genetics, Japan):*E. coli* for providing plasmids and strains from the ASKA and KEIO collections respectively. We are grateful to Pierre Dehoux (PF4, Institut Pasteur) for sequence comparisons between YncC and regulators of the GntR family.

‡ To whom correspondence should be addressed : Institut Pasteur, Unité de Génétique Moléculaire; URA-CNRS 2172; 25 rue du Docteur Roux, 75724 Paris Cedex 15, France. Tel.: 33-140613122; Fax: 33- 145688960; E-mail: francoise.norel@pasteur.fr.

REFERENCES

- Gruber, T.M., and Gross, C.A. (2003) Multiple sigma subunits and the partitioning of bacterial transcription space. *Annu. Rev. Microbiol.* **57**, 441–466
- Ishihama, A. (2000) Functional modulation of *Escherichia coli* RNA polymerase. *Annu. Rev. Microbiol.* **54**, 499–518
- Klauck, E., Typas, A., and Hengge, R. (2007) The sigmaS subunit of RNA polymerase as a signal integrator and network master regulator in the general stress response in *Escherichia coli*. *Sci. Prog.* **90**, 103–127
- Dong, T., and Schellhorn, H. E. (2010) Role of RpoS in virulence of pathogens. *Infect. Immun.* **78**, 887–897
- Bang, I.S., Frye, J.G., McClelland, M., Velayudhan, J., and Fang, F.C. (2005) Alternative sigma factor interactions in *Salmonella*: sigmaE and sigmaH promote antioxidant defences by enhancing sigmaS levels. *Mol. Microbiol.* **56**, 811–823
- Weber, H., Polen, T., Heuveling, J., Wendisch, V. F., and Hengge, R. (2005) Genome-wide analysis of the general stress response network in *Escherichia coli*: sigmaS-dependent genes, promoters, and sigma factor selectivity. *J. Bacteriol.* **187**, 1591–1603
- Ibanez-Ruiz, M., Robbe-Saule, V., Hermant, D., Labrude, S., and Norel, F. (2000) Identification of RpoS (sigma(S))-regulated genes in *Salmonella enterica* serovar Typhimurium. *J. Bacteriol.* **182**, 5749–5756
- Rigali, S., Derouaux, A., Giannotta, F., and Dusart, J. (2002) Subdivision of the helix-turn-helix GntR family of bacterial regulators in the FadR, HutC, MocR, and YtrA subfamilies. *J. Biol. Chem.* **277**, 12,507–12,515
- Hoskisson, P.A., and Rigali, S. (2009) Chapter 1: Variation in form and function of the helix-turn-helix regulators of the GntR superfamily. *Adv. Appl. Microbiol.* **69**, 1–22
- Xu, Y., Heath, R. J., Li, Z., Rock, C. O., and White, S. W. (2001) The FadR-DNA complex. Transcriptional control of fatty acid metabolism in *Escherichia coli*. *J. Biol. Chem.* **276**, 17373–17379
- Poon, T. C. (2007) Opportunities and limitations of SELDI-TOF-MS in biomedical research: practical advices. *Expert Rev. Proteomics.* **4**, 51–65
- Robbe-Saule, V., Coynault, C., Ibanez-Ruiz, M., Hermant, D., and Norel, F. (2001) Identification of a non-haem catalase in *Salmonella* and its regulation by RpoS (sigmaS). *Mol. Microbiol.* **39**, 1533–1545
- Zhang, X. S., Garcia-Contreras, R., and Wood, T. K. (2008) *Escherichia coli* transcription factor YncC (McbR) regulates colanic acid and biofilm formation by repressing expression of periplasmic protein YbiM (McbA). *ISME J.* **2**, 615–631
- Dorman, C. J. (2007) H-NS, the genome sentinel. *Nat. Rev. Microbiol.* **5**, 157–161
- Fang, F. C., and Rimsky, S. (2008) New insights into transcriptional regulation by H-NS. *Curr. Opin. Microbiol.* **11**, 113–120
- Dorman, C. J., and Kane, K. A. (2009) DNA bridging and anti-bridging: a role for bacterial nucleoid-associated proteins in regulating the expression of laterally acquired genes. *FEMS Microbiol. Rev.* **33**, 587–592
- Sambrook, J., Fritsch, E. F., and Maniatis, T. (1989) *Molecular cloning: A Laboratory Manual* (2nd ed.), Cold Spring Harbor, N. Y.
- Blattner, F. R., Plunkett, G., 3rd, Bloch, C. A., Perna, N. T., Burland, V., Riley, M., Collado-Vides, J., Glasner, J. D., Rode, C. K., Mayhew, G. F., Gregor, J., Davis, N. W., Kirkpatrick, H. A., Goeden, M. A., Rose, D. J., Mau, B., and Shao, Y. (1997) The complete genome sequence of *Escherichia coli* K-12. *Science.* **277**, 1453–1462
- Bertin, P., Terao, E., Lee, E. H., Lejeune, P., Colson, C., Danchin, A., and Collatz, E. (1994) The H-NS protein is involved in the biogenesis of flagella in *Escherichia coli*. *J. Bacteriol.* **176**, 5537–5540
- Baba, T., Ara, T., Hasegawa, M., Takai, Y., Okumura, Y., Baba, M., Datsenko, K. A., Tomita, M., Wanner, B. L., and Mori, H. (2006) Construction of *Escherichia coli* K-12 in-frame, single-gene knockout mutants: the Keio collection. *Mol. Syst. Biol.* **2**, 2006.0008
- Robbe-Saule, V., Lopes, M.D., Kolb, A., and Norel, F. (2007) Physiological effects of Crl in *Salmonella* are modulated by sigmaS level and promoter specificity. *J. Bacteriol.* **189**, 2976–2987
- Robbe-Saule, V., Jaumouillé, V., Prévost, M. C., Guadagnini, S., Talhouarne, C., Mathout, H., Kolb, A., and Norel, F. (2006) Crl activates

- transcription initiation of RpoS-regulated genes involved in the multicellular behavior of *Salmonella enterica* serovar Typhimurium. *J. Bacteriol.* **188**, 3983–3994
23. Chang, A. C., and Cohen, S. N. (1978) Construction and characterization of amplifiable multicopy DNA cloning vehicles derived from the P15A cryptic miniplasmid. *J. Bacteriol.* **134**, 1141–1156
 24. Kitagawa, M., Ara, T., Arifuzzaman, M., Ioka-Nakamichi, T., Inamoto, E., Toyonaga, H., and Mori, H. (2005) Complete set of ORF clones of *Escherichia coli* ASKA library (a complete set of *E. coli* K-12 ORF archive): unique resources for biological research. *DNA Res.* **12**, 291–299
 25. Marschall, C., Labrousse, V., Kreimer, M., Weichart, D., Kolb, A., and Hengge-Aronis, R. (1998) Molecular analysis of the regulation of *csiD*, a carbon starvation-inducible gene in *Escherichia coli* that is exclusively dependent on sigma S and requires activation by cAMP-CRP. *J. Mol. Biol.* **276**, 339–353
 26. Schmieger, H. (1972) Phage P22-mutants with increased or decreased transduction abilities. *Mol. Gen. Genet.* **119**, 75–88
 27. Sternberg, N. L., and Maurer, R. (1991) Bacteriophage-mediated generalized transduction in *Escherichia coli* and *Salmonella typhimurium*. *Methods Enzymol.* **204**, 18–43
 28. Silhavy, T. J., Bernman, M. L., and Ernqvist, L. W. (1984) *Experiments with Gene Fusions*, Cold Spring Harbour, N. Y.
 29. Jarvik, T., Smillie, C., Groisman, E. A., and Ochman, H. (2010) Short-term signatures of evolutionary change in the *Salmonella enterica* serovar Typhimurium 14028 genome. *J. Bacteriol.* **192**, 560–567
 30. Datsenko, K. A., and Wanner, B. L. (2000) One-step inactivation of chromosomal genes in *Escherichia coli* K-12 using PCR products. *Proc. Natl. Acad. Sci. U.S.A.* **97**, 6640–6645
 31. Ellermeier, C. D., Janakiraman, A., and Slauch, J. M. (2002) Construction of targeted single copy *lac* fusions using lambda Red and FLP-mediated site-specific recombination in bacteria. *Gene.* **290**, 153–161
 32. Miller, J. H. (1972) *Experiments in Molecular Genetics*, Cold Spring Harbour, N. Y.
 33. Coynault, C., Robbe-Saule, V., and Norel, F. (1996) Virulence and vaccine potential of *Salmonella typhimurium* mutants deficient in the expression of the RpoS (sigma S) regulon. *Mol. Microbiol.* **22**, 149–160
 34. Depardieu, F., Courvalin, P., and Kolb, A. (2005) Binding sites of VanRB and sigma70 RNA polymerase in the *vanB* vancomycin resistance operon of *Enterococcus faecium* BM4524. *Mol. Microbiol.* **57**, 550–564
 35. Maxam, A. M., and Gilbert, W. (1977) A new method for sequencing DNA. *Proc. Natl. Acad. Sci. U.S.A.* **74**, 560–564
 36. Huo, Y. X., Tian, Z. X., Rappas, M., Wen, J., Chen, Y. C., You, C. H., Zhang, X., Buck, M., Wang, Y. P., and Kolb, A. (2006) Protein-induced DNA bending clarifies the architectural organization of the sigma54-dependent *glnAp2* promoter. *Mol. Microbiol.* **59**, 168–180
 37. Monteil, V., Kolb, A., D'Alayer, J., Beguin, P., and Norel, F. (2010) Identification of conserved amino acid residues of the *Salmonella* sigmaS chaperone Crl involved in Crl-sigmaS interactions. *J. Bacteriol.* **192**, 1075–1087
 38. Lawrence, J. G., and Ochman, H. (1998) Molecular archaeology of the *Escherichia coli* genome. *Proc. Natl. Acad. Sci. U.S.A.* **95**, 9413–9417
 39. Lucchini, S., Rowley, G., Goldberg, M. D., Hurd, D., Harrison, M., and Hinton, J. C. (2006) H-NS mediates the silencing of laterally acquired genes in bacteria. *PLoS Pathog.* **2**, e81
 40. Navarre, W. W., Porwollik, S., Wang, Y., McClelland, M., Rosen, H., Libby, S. J., and Fang, F. C. (2006) Selective silencing of foreign DNA with low GC content by the H-NS protein in *Salmonella*. *Science.* **313**, 236–238
 41. Chan, K., Baker, S., Kim, C. C., Detweiler, C. S., Dougan, G., and Falkow, S. (2003) Genomic comparison of *Salmonella enterica* serovars and *Salmonella bongori* by use of an *S. enterica* serovar Typhimurium DNA microarray. *J. Bacteriol.* **185**, 553–563
 42. Zhou, Y., and Gottesman, S. (2006) Modes of regulation of RpoS by H-NS. *J. Bacteriol.* **188**, 7022–7025
 43. Yoshida, T., Ueguchi, C., Yamada, H., and Mizuno, T. (1993) Function of the *Escherichia coli* nucleoid protein, H-NS: molecular analysis of a subset of proteins whose expression is enhanced in a *hns* deletion mutant. *Mol. Gen. Genet.* **237**, 113–122
 44. Lang, B., Blot, N., Bouffartigues, E., Buckle, M., Geertz, M., Gualerzi, C. O., Mavathur, R., Muskhelishvili, G., Pon, C. L., Rimsky, S., Stella, S., Babu, M. M., and Travers, A. (2007) High-affinity DNA binding sites for H-NS provide a molecular basis for selective silencing within proteobacterial genomes. *Nucleic Acids Res.* **35**, 6330–6337
 45. Stoebel, D. M., Free, A., and Dorman, C. J. (2008) Anti-silencing: overcoming H-NS-mediated repression of transcription in Gram-negative enteric bacteria. *Microbiology.* **154**, 2533–2545
 46. Browning, D. F., and Busby, S. J. (2004) The regulation of bacterial transcription initiation. *Nat. Rev. Microbiol.* **2**, 57–65
 47. Espinosa-Urgel, M., and Tormo, A. (1993) Sigma S-dependent promoters in *Escherichia coli* are located in DNA regions with intrinsic curvature. *Nucleic Acids Res.* **21**, 3667–3670
 48. Typas, A., Barembuch, C., Possling, A., and Hengge, R. (2007) Stationary phase reorganisation of the *Escherichia coli* transcription machinery by Crl protein, a fine-tuner of sigmaS activity and levels. *EMBO J.* **26**, 1569–1578
 49. Radde, N., Gebert, J., Faigle, U., Schrader, R., and Schnetz, K. (2008) Modeling feedback loops in the H-NS-mediated regulation of the *Escherichia coli* *bgl* operon. *J. Theor. Biol.* **250**, 298–306
 50. Osborne, S. E., Walthers, D., Tomljenovic, A. M., Mulder, D. T., Silphaduang, U., Duong, N., Lowden, M. J., Wickham, M. E., Waller, R. F., Kenney, L. J., and Coombes, B. K. (2009) Pathogenic adaptation of intracellular bacteria by rewiring a *cis*-regulatory input function. *Proc. Natl. Acad. Sci. U.S.A.* **106**, 3982–3987
 51. Perez, J. C., and Groisman, E. A. (2009) Transcription factor function and promoter architecture govern the evolution of bacterial regulons. *Proc. Natl. Acad. Sci. U.S.A.* **106**, 4319–4324
 52. Perez, J. C., and Groisman, E. A. (2009) Evolution of transcriptional regulatory circuits in bacteria. *Cell.* **138**, 233–244
 53. Hindupur, A., Liu, D., Zhao, Y., Bellamy, H. D., White, M. A., and Fox, R. O. (2006) The crystal structure of the *E. coli* stress protein YciF. *Protein Sci.* **15**, 2605–2611
 54. Hébrard, M., Viala, J. P., Méresse, S., Barras, F., and Aussel, L. (2009) Redundant hydrogen peroxide scavengers contribute to *Salmonella* virulence and oxidative stress resistance. *J. Bacteriol.* **191**, 4605–4614
 55. Ryu, J. H., Ha, E. M., Oh, C. T., Seol, J. H., Brey, P. T., Jin, I., Lee, D. G., Kim, J., Lee, D., and Lee, W. J. (2006) An essential complementary role of NF-kappaB pathway to microbicidal oxidants in *Drosophila* gut immunity. *EMBO J.* **25**, 3693–3701